Rotation-aged genetic parameters for shortleaf pine (Pinus echinata Mill.) and their implications for tree improvement, disturbance response, and species restoration in a changing climate

Chen Ding

czd0084@auburn.edu

Auburn University System

Shaik M. Hossain

Alabama A&M University

Yuhui Weng

Stephen F. Austin State University

Hao Chen

Auburn University System

Barbara S. Crane

US Forest Service

Earl M. (Fred) Raley

Texas AM Forest Service

Don C. Bragg

US Forest Service

C. Dana Nelson

US Forest Service

Research Article

Keywords: Pinus echinata, additive genetic variance, height, DBH, survival, ice damage, genetic gain, genotype-by-environment interaction

Posted Date: June 8th, 2026

DOI: https://doi.org/10.21203/rs.3.rs-9765483/v1

Additional Declarations: No competing interests reported.

Rotation-aged genetic parameters for shortleaf pine (*Pinus echinata* Mill.) and their implications for tree improvement, disturbance response, and species restoration in a changing climate

Chen Ding[1,2], Shaik M. Hossain[3], Yuhui Weng[4], Hao Chen[2], Barbara S. Crane[5*], Earl M. Raley[1], Don C. Bragg[6**], and C. Dana Nelson[7,8*]

[1]Western Gulf Forest Tree Improvement program, Texas AM Forest Service, TAMU, College Station, TX 77843, USA;
[2] College of Forestry, Department of Wildlife and the Environment, Auburn University, Auburn, AL 36849, USA;
[3] Forestry, Ecology and Wildlife Program, Department of Natural Resources, Biological and Environmental Sciences, Alabama A&M University, Normal, AL 35762, USA;
[4] Arthur Temple College of Forestry and Agriculture, Stephen F. Austin State University, Nacogdoches, TX 75962, USA;
[5] USDA Forest Service, Southern Region, Atlanta, GA 30309, USA;
[6] USDA Forest Service, Southern Research Station, Monticello, AR 71655, USA;
[7] USDA Forest Service, Southern Research Station, Forest Health Research and Education Center, Lexington, KY 40546, USA;
[8] USDA Forest Service, Southern Research Station, Southern Institute of Forest Genetics Saucier, MS 39574, USA; Department of Forestry and Natural Resources, University of Kentucky, Lexington, KY 40546, USA
[*] retired, Emeritus Scientist
[**] deceased

Corresponding authors: Chen DING czd0084@auburn.edu
C. Dana Nelson

Article type: Research Article

Article length: Abstract: 356 words, main text: 7753 words
References: 62, Tables: 2, and Figures: 6

Keywords: *Pinus echinata*, additive genetic variance, height, DBH, survival, ice damage, genetic gain, genotype-by-environment interaction

Abstract

Understanding the adaptation to extreme weather events in long-lived conifers while maintaining a competitive growth rate has become increasingly critical for tree improvement focused on successful reforestation and ecosystem restoration. We investigated the genetic parameters of shortleaf pine (*Pinus echinata* Mill), a wide-ranging but declining conifer of the southern USA, by analyzing survival, height and diameter growth, stem taper, and ice storm damage using progeny trial data collected through typical economic rotation ages (30 to 40 years). We evaluated 15 progeny trials representing 330 full-sib families formed by a series of disconnected half-diallel crosses among 150 parents originating from three seed-source regions (East Ouachita, West Ouachita, and Ozark) within two environmental zones (Ouachita Mountains and Ozark Plateau) and tested in each zone. Both individual tree- and family-based statistical models provided robust genetic parameter estimates. Narrow-sense heritability of tree height increment from age-5 years to the rotation-age measurement reached 0.38 across the trials that were not impacted by a particularly severe, mid-rotation ice storm. Only negligible dominance genetic and genotype-by-environment variance for growth traits were observed in these trials. Low to moderate genetic control (narrow-sense heritability of 0.1-0.4) suggests that appreciable genetic gain of stem volume (function of tree height and stem diameter) and stem taper are achievable. Genetic correlations were generally favorable among traits, although when not, "correlation breaker" parents could be identified and selected to obtain gain in both volume and tolerance (i.e., resiliency) to ice damage. Despite variations in the impact of the severe ice storm across the trials, our results revealed significant and biologically important levels of genetic control for all traits. Trials that were most severely affected by the severe ice storm presented a unique opportunity for selecting individuals with increased tolerance to ice damage. No discernable trade-off between growth and tolerance to ice damage was found, as faster growing genotypes tended to recover from ice storm damage quickly, thereby maintaining their growth and size advantage in the stands. Overall, our results underscore the potential of tree improvement for enhancing the genetic potential of shortleaf pine and contributing to the success of ongoing reforestation and ecosystem restoration efforts across the southern USA.

1. Introduction

Reforestation and restoration of forested ecosystems play critical roles for global economies and terrestrial carbon sequestration with plantation forests alone reaching 313 million ha globally (FAO, 2025). However, tree species with wide habitat ranges encounter elevated maladaptation risks due to the heterogeneous site conditions and productivity loss associated with inter-specific and intra-specific genetic miss-matches (Aitken *et al. 2*008; Alberto *et al. 2*013; Tyrmi *et al. 2*020). Excessive mortality and productivity losses due to maladaptation pose significant threats to the sustainability of forests as well as economic resilience of local communities. Elevated frequency, intensity and severity of extreme weather events associated with climate change have resulted in more pronounced and even catastrophic impacts (Wuebbles *et al. 2*014; Rustad *et al. 2*020; Intergovernmental Panel on Climate Change, 2023). The escalation of extreme, episodic weather such as unseasonal freezes and severe ice storms will threaten different forest types, including those planted for forestry production as well as for ecosystem restoration (Arora and Taulavuori, 2016).

Local adaptations are commonly observed in naturally regenerating tree populations, with diverse abiotic and biotic factors influencing both phenotypic and genetic variations in adaptive and productivity traits (Keller *et al. 2*011; Wang *et al. 2*014; Zhang *et al. 2*019; Ding and Brouard, 2022; Hu *et al. 2*022). Maladaptation, when present, and associated tree mortality are related to multiple abiotic and biotic stresses exacerbated by the increasing frequency of extreme weather conditions (Worrall *et al. 2*013; Anderegg *et al. 2*015; Aitken and Bemmels 2016; Ware *et al. 2*021; Leuschner *et al. 2*023). To address this situation, tree improvement provides the needed testing of populations for adaptability and productivity under current and projected future environmental conditions. Clearly, ensuring adaptability to increasing extreme weather events while maintaining competitive growth increments for long-lived tree species is critical for successful reforestation efforts, including species and ecosystem restoration. As a precursor to tree improvement, provenance tests (seed source or common garden studies) are often conducted on multiple sites to investigate genetic and genetic × environmental responses of survival and growth traits. These studies are critically important as they provide information on associations

between phenotypes, genotypes, and environments, where climate variables at the source location of the genotypes and test planting locations are considered (Rehfeldt *et al.*, 1999; Isabel *et al. 2*020; Ye *et al. 2*023).

Extreme weather or disturbance events can shrink genetic variations of adaptive traits through a strong selection event, such as unseasonable freezes, heavy ice storms, insect or disease outbreaks, extended periods of drought, damaging windstorms, and unusual fire events (Szmyt and Dering, 2024). Foresters and tree breeders often abandon common garden trials when mortality reaches a threshold (e.g., >~30%), potentially missing an opportunity to study longer-term adaptive traits. Long-standing trials carried out to or beyond rotation-ages can create an opportunity for studying natural adaptation and selection of responses across the full spectrum of stand development. This is especially relevant for both seasonal and unseasonal extreme (acute) stresses such those mentioned above. For example, prolonged drought causes accumulated (chronic) functional declines of susceptible trees, families, and seed sources (Anderegg *et al. 2*013). Genetic trials monitored through rotation age provide the "data log" needed to evaluate trees through acute and chronic stress events (Montwe *et al. 2*018).

A previous landscape-scale study (~8,700m^2) in Europe demonstrated that the drivers of ice storm damage include storm intensity, site elevation, tree species, and lesser important factors including tree DBH and status in the stand, species diversity indices, and slope of the site (Klopčič *et al. 2*019). *Pinus* species were found to be the most susceptible to the ice storms among multiple conifer and hardwood species (Klopčič *et al. 2*019). Mechanical damage of tree branches and the main leaders were associated with the frequency and severity of the ice storm and the extent of freezing after the storm (Rustad *et al. 2*020). Stem defects caused by multiple stress episodes, especially mechanical breakage, significantly reduced the sawlog values of surviving trees (Katrevics *et al. 2*020). The potential for genetic improvement of traits such as tolerance to ice damage is unknown due to the limited availability of long-term field performance data of appropriate genetic materials. However, Hossain *et al.* (2021) reported that following a severe ice storm, surviving shortleaf pine exhibited a diagnostic injury (i.e., a visual crook) to their main stems that could be used to score ice damage and evaluate the trees' post-damage growth response.

Genetic parameters including genetic variances and covariances and resulting heritability and genetic correlation estimates of measured traits inform and guide the tree improvement programs toward the development of high performing planting stock (Ding and Brouard 2022; Ding *et al. 2*023). Additive genetic variance and narrow-sense heritability are of interest to predict the genetic gain from selection, while mating-designs such as the diallel and partial diallel provide half-sib and full-sib families needed to estimate these parameters and the potential for genetic gains (Jansson and Li, 2004b; Dong *et al. 2*019). Genetic parameters including heritability, type-B genetic correlations, general (GCA) and the specific combining abilities (SCA) have been estimated in previous studies for many *Pinus* species (Wu and Matheson 2001 ; Xiang *et al. 2*003b ; Jansson and Li, 2004a; Baltunis *et al. 2*005 ; McKeand *et al. 2*008), providing rich resources of the genetic parameters of growth traits. A typical range of narrow-sense heritability of height and DBH range from 0.1-0.2 (i.e., 10 to 20%) in the diallel studies (Xiang *et al. 2*003b; McKeand *et al. 2*008), while dominance variance is limited to no more than about 6% of total phenotypic variance for height and volume (McKeand *et al. 2*008). Clonal mean heritability of volume of loblolly pine was 0.4, with a boost of estimate to 0.6 when using complex statistical models (Shalizi, 2020).

For a shortleaf pine population tested on multiple sites, Hossain *et al.* (2021) reported that the individual-tree heritability was 0.15, 0.1, and 0.07 for DBH, height, and survival, respectively, suggesting that genetic gains through selection could be made. However, their study did not include the estimation of narrow-sense heritability or individual or parent tree breeding values for direct application in tree improvement. Mating designs (e.g., diallels including full or half, and disconnected diallels) allow the estimates of general (GCA) and specific combining abilities (SCA) (McKeand *et al. 2*008; Isik *et al. 2*017), so the additive and non-additive genetic effects (i.e., dominance genetic effect) are exploitable for improving genetic gains in tree improvement (Dong et al. 2020). Backward selection can increase the genetic gain of seed orchard families after roguing the inferior families while maintaining superior families, while forward selection screens the best individuals/progenies of the half-sib or full-sib families for the genetic improvement of the next generations (Li *et al. 2*024). The interaction between GCA and environment can be addressed with multi-environment tests (McKeand *et al. 2*008) that allows the evaluation of the stability of genetic performance at various plantation sites.

Genetic parameters, i.e., GCA and SCA, correlations between traits, and breeding values will inform tree improvement by enabling efficient selection strategies to be developed. In this study, we focused on backward selection for operations such as seed orchard roguing to improve existing orchards. Future work may incorporate forward selection for the purpose of developing new seed orchards.

Robust experimental design is efficiently employed for common garden experiments, including progeny tests using the pedigrees created by the mating designs and randomized complete or incomplete blocking designs to control for environmental effects across field sites. In addition, spatial adjustments can dissect the spatially correlated variations from the random residuals and *post-hoc* adjustment such as row-column have also been shown to be useful for improving genetic parameter estimates in forest trees (Gezan *et al. 2*006a; Zhang *et al. 2*015; Shalizi and Isik, 2019; Ding *et al. 2*023). The microsite heterogeneity and random "noise" in the environmental variances can be addressed and properly quantified using these analytical techniques. Accounting for and adjusting the spatial effects by row-column modeling and incomplete blocking improved the genetic parameter estimates for historically constructed progeny common garden trials (Ding *et al. 2*023).

Shortleaf pine (*Pinus echinata* Mill.), an ecologically and economically important species that often co-occurs with loblolly pine (*Pinus taeda* L.), is under considerable threat with significant declines across its range in the southeastern USA (Stewart *et al. 2*016; Hossain *et al. 2*021). The species plays a keystone role in several forest types and many ecosystems where fire is relatively frequent on the landscape (Stewart *et al. 2*016). However, the genetics and ecology of shortleaf pine have not been broadly investigated, including its ecological adaptations and traits important to stand productivity (Stewart *et al. 2*016). Shortleaf pine is typically managed for sawlog production and planted for ecosystem restoration at colder and drier sites compared to those managed for loblolly pine.

In the current study, we evaluated the correlated response of ice storm damage and tree growth through rotation-age in multi-environment progeny trials (MET) of shortleaf pine. A series of disconnected half-diallels were used to establish the MET in the Ouachita Mountains and Ozark Highlands of northwest Arkansas, USA. The MET was established in this region to

provide a focal view of the genetic, environment, and genetic x environment interaction of a major shortleaf pine seed source managed within the genetic resources program of the USDA Forest Service. Our study objectives included: 1) estimating genetic parameters (heritability, genetic correlations, breeding values) using multiple statistical models after adjusting for within-site spatial autocorrelations and planting site effects; 2) investigating how extreme weather events, such as a severe ice storm serves as a potential selection factor in METs using multiple genetic parameters; and 3) projecting the correlated response of ice damage tolerance after selecting for increased tree height and volume growth at rotation age.

2. Materials and methods

2.1. Study area of seed sources and test sites

The shortleaf pine progeny tests of the USDA Forest Service's (USDA-FS) Southern Region cover the complete span of the Ouachita National Forest in Arkansas and Oklahoma and the Ozark-St. Francis National Forest in northern Arkansas. The Ouachita Mountains are characterized by folded ridges and valleys composed of Paleozoic rocks (Woods *et al. 2*004). The ridges are generally aligned east to west, resulting in extensive south-facing slopes that are exposed to sunlight and becomes dry and north-facing slopes that are protected from direct solar radiation and are consequently cooler and more mesic. This topographic orientation generates different forest vegetation bands, with south-facing slopes supporting xeric shortleaf pine and pine–oak woodlands, while north-facing slopes favor mesic hardwood forests where shortleaf pine is frequently absent, reflecting microclimatic filtering. Annual precipitation in the Arkansas Ouachita Mountains ranges from 1,200 mm to 1,400 mm. The mean minimum (January) and maximum (July) monthly temperatures in the Ouachitas are 8.7°C and 22.0°C, respectively (PRISM Climate Group; Pugh and Westerman, 2014). The Ozark Mountains are characterized by flat-topped plateaus, rugged hills, and deep valleys carved by streams into the limestone and dolomite bedrock that underlies most of the area. The Ozarks are comprised of three distinct plateaus —Boston, Springfield, and Salem—each representing a slightly different vegetation type (Woods *et al. 2*004). Like the Ouachita Mountains, the warm south-facing Ozark slopes are dominated by xeric shortleaf pine and shortleaf pine-oak forests, and cool, north-facing slopes are mostly mesic oak-hickory forests. Average minimum and maximum monthly (January and

July) temperatures in the Ozarks are 7.1°C and 20.2 °C, respectively, while annual precipitation ranges from 1,100 mm to 1,400 mm (PRISM Climate Group). To summarize and explore the climatic space and growth correlation of the progeny trials, we employed principal component analysis (PCA) and constructed the principal components (PCs) with the R function *pcomp()*.

2.2. Seed source and families, half diallel mating design, provenance test, and data collections

The parent trees for the shortleaf pine progeny tests were selected from three then-designated provenances or seed zones within the Ouachita and Ozark-St. Francis National Forests: East Ouachita (EOU), West Ouachita (WOU), and Ozark (OZ) (Fig. 1). Details of the long-term progeny tests used in this study, were previously documented by Hossain et al. (2021). The trial employed a six-by-six disconnected half-diallel mating design, incorporating parents from three seed provenances. In the mating design, parents from all three zones were used as female and male parents using 25 crossing groups (half-diallel). This design generated 375 full-sib families from 150 parents, comprising both intra-provenance crosses (within the same zone) and inter-provenance crosses (between different zones).

Seeds from these controlled crosses were planted across the seedzones and 15 field tests were analyzed as a subset of more than 39 tests planted due to a balanced sampling of tests per seedzone, accessibility, and completed documentation of re-measurement from seedlings to the rotation age (Hossain et al. 2021). Over the trials' 31- to 40-year measurement period, which included a severe ice storm in December 2000 (test ages 12 to 22 years), the dataset was consolidated into 330 re-measured full-sib families and 126 half-sib families. Most full-sib families (249) were unique to a single test location, while 88 were shared between two locations, and only 8 were found in three or more (Hossain et al. 2021). The transplant provenance variance of the regions (e.g., EOU provenance tested at WOU trial sites) was tested in the genetic analysis and found not to be significant, so we ignored this term in the formal analysis. From the seed source perspective, we focused on the geographical factors related to the ice storm's damage (i.e., 11 tests were in the ice-damaged area and 4 were not) and the recovery of the trees after the storm.

For ice storm damage, live trees were categorized as either damaged in the 2000 ice storm (e.g., typically presenting with an obvious "crook" in the upper stem) or undamaged (Hossain et

al. 2021). A simple condition and status assessment of both live (e.g., ice damage, fork defect, and insect damage) and dead trees (e.g., dead standing, dead and down, and dead missing) was recorded. For each test, test age at measurement time was determined as the planting year subtracted from the measurement year, since tests were planted and measured in different years.

The number of full-sib families per test location ranged from 25 to 37 of the 330 total full-sib families tested, with 113 families in the EOU tests, 82 families in the OZ tests, and 55 families in the WOU tests. Although the tests were established on multiple sites in each zone (EOU, WOU, and OZ), most of the full-sib families were only tested on one site. We estimated G×E for additive genetic effects using the linear mixed model, which provides estimates of type-B genetic correlations. Due to the structure of the disconnected half-diallel design, reciprocal effect variances were not estimable. Within the family model, we specifically evaluated the female parent × environment interaction. Preliminary analyses indicated that the male family × environment and tree age × test site interaction terms were non-significant; so, both were excluded from the final models.

2.3. Row and column *post-hoc* analyses

Due to the spatially related within-site environmental variation we used *post-hoc* adjustments to better account for variations on micro-site scale and across experimental design replicates (Gezan *et al. 2*006a; Gezan *et al. 2*006b; Xing *et al. 2*017; Ding *et al. 2*023). We applied the existing RCBD row plot information and the continuous row, column (meters) coordinates based on the original maps (Ding *et al. 2*023). All missing and filler trees were counted to create the complete trial map though only surviving trees were counted in the analyses (Table 1). Thus, in the *post-hoc* analyses*,* within each original RCBD block, the incomplete blocks, i.e., rows and columns, contain 25-60 rows, 25-148 columns, and 5-6 trees per row-plot for the 15 trials. To address potential biases resulting from variable micro-environmental conditions, *post-hoc* analysis using a row-column design was conducted to improve the estimates of genetic parameters.

2.4. Tree volume and taper estimates

We applied the following volume functions for the individual trees. Complete volume of stem-wood and -bark (m^3, VOL = 0.00006* DBH **2.2186* HT**0.6261), and the complete green weight of stem-wood and -bark (kg, WT = 0.0432* DBH**2.0702* HT**0.8828) (Coble *et al.*

*2*004). Taper of individual trees was calculated as TPR = DBH *(1.07996+0.28760* log(1-0.9776*(1.3/HT)**(1/3))) (Tiarks and Baldwin JR, 1999).

2.5. Linear mixed model analysis

Multiple linear mixed models (MLMM) were employed for predicting the breeding values of female families: (1) single-site analyses to estimate the breeding values; (2) combined analyses (MET) considering both age and row-column effects; (3) multi-variate analyses of traits by adjusting for age effects. Single-site analyses were not reported in detail here due to similar trends as in the MET analyses and relatively higher standard errors of variance components due to smaller sample sizes.

The basic MLMM is

$$y = X\beta + Z_1 a + Z_2 ae + Z_3 d + Z_4 de + Z_5 r + e \quad (1)$$

where, the fixed effect is **β** including the age effect, environmental zone effect, site effect nested in age and zones, row effect and column effect nested within the test-age-zone respectively; block nested within test-age-zone; the zone transfer (moving between zones) of male and female parent were not fitted in the fixed effect due to the insignificance; *a* denotes the random vector of additive genetic effect, with a$\sim N(0, \sigma_A^2 A)$, where σ_A^2 is the additive genetic variance and *A* is the pedigree kinship matrix; *d* denotes the random vector of dominance genetic effect, with d$\sim N(0, \sigma_D^2 D)$, where σ_D^2 is the dominance genetic variance and *D* is the dominance relationship matrix; *ae* is the random additive genetic-by-environment interaction effect with ae$\sim N(0, \sigma_{ae}^2 \otimes I)$; *de* is the random dominance genetic-by-environment interaction effect with de$\sim N(0, \sigma_{de}^2 \otimes I)$; r is the random row plot effect nested in the trial r $\sim N\left(0, \sigma_{r(t)}^2 \otimes I\right)$, where t is the t^{th} block-progeny test site-age-zone combination; Z_1 to Z_5 denote the incidence design matrices relating following random effects *a*, *ae*, *d*, *de*, *r*, respectively, to observations *Y*. Post hoc factors were not used as random factors in the multiple environment trial analyses. The total variance matrix can be partitioned into components based on the vectors of random effects mentioned previously as follows,

$$V = \sigma_A^2 Z_1 A Z_1' + \sigma_{ae}^2 Z_2 Z_2' + \sigma_D^2 Z_3 Z_3' + \sigma_{de}^2 Z_4 Z_4' + \sigma_{r(t)}^2 Z_5 Z_5' + R \quad (2)$$

The best linear unbiased estimation (BLUE) of fixed effect (β) and best linear unbiased prediction (BLUP) of random effects (*a, r, ae, row, column*) are solutions to the following mixed model equations,

$$\begin{bmatrix} \hat{\beta} \\ \hat{a} \\ \widehat{ae} \\ \hat{d} \\ \widehat{de} \\ \widehat{r(t)} \end{bmatrix} =$$

$$\begin{bmatrix} I'I & I'Z_1 & I'Z_2 & I'Z_3 & I'Z_4 & I'Z_5 \\ Z_1'I & Z_1'Z_1 + A^{-1}\frac{\widehat{\sigma_E}^2}{\widehat{\sigma_A}^2} & Z_1'Z_2 & Z_1'Z_3 & Z_1'Z_4 & Z_1'Z_5 \\ Z_2'I & Z_2'Z_1 & Z_2'Z_2 + I_{ae}\frac{\widehat{\sigma_E}^2}{\widehat{\sigma_{AE}}^2} & Z_2'Z_3 & Z_2'Z_4 & Z_2'Z_5 \\ Z_3'I & Z_3'Z_1 & Z_3'Z_2 & Z_3'Z_3 + D^{-1}\frac{\widehat{\sigma_E}^2}{\widehat{\sigma_D}^2} & Z_3'Z_4 & Z_3'Z_5 \\ Z_4'I & Z_4'Z_1 & Z_4'Z_2 & Z_4'Z_3 & Z_4'Z_4 + I_{de}\frac{\widehat{\sigma_E}^2}{\widehat{\sigma_{DE}^2}} & Z_4'Z_5 \\ Z_5'I & Z_5'Z_1 & Z_5'Z_2 & Z_5'Z_3 & Z_5'Z_4 & Z_5'Z_5 + I_{rt}\frac{\widehat{\sigma_E}^2}{\widehat{\sigma_{rt}^2}} \end{bmatrix}^{-1} \begin{bmatrix} I'Y \\ Z_1'Y \\ Z_2'Y \\ Z_3'Y \\ Z_4'Y \\ Z_5'Y \end{bmatrix}$$

(3)

Eleven of the 15 trials were impacted by the severe ice storm (December 2000, test ages 12 to 22). The four non-impacted trials were all in the OZ zone as this ice storm passed to the south of the Ozark zone (Table 1). The linear model for ice damage is similar as (1) with details in the (A1 in supplementary materials). For MET analyses, heterogeneous variance, and nearest neighbor variance had two dimensional first-order autoregressive (x and y, AR1) variance of residual; the details are also listed in the supplementary materials. Another univariate family (general combining ability-GCA, specific combining ability-SCA) models were constructed for estimating other family heritabilities with family terms (A2 in supplementary materials) comparing to the individual tree models (A1 in supplementary materials).

The multivariate BLUP was employed to estimate the correlations between traits, i.e., additive genetic correlation and phenotypic correlations. We ran all pairs of traits in ASReml -R Ver. 3.0. The bivariate mixed model is as follows,

$$\begin{pmatrix} y_1 \\ y_2 \end{pmatrix} = X\beta + Z_1 a(t) + Z_2 d(t) + e \quad (4)$$

where y_1 and y_2 are the vectors of phenotypic observations for traits 1 and 2 respectively; β is the vector of the fixed effects including an overall mean of each trait: age, age-trait interaction, zone, zone within trait, rep within age and within trial and within zone (i.e., EOU, WOU, and OZ); a(t) is the random additive genetic effect within trait, with a(t)$\sim N(0, V_A \otimes A)$; and d(t) is the random dominance genetic effect within trait, with d(t)$\sim N(0, V_D \otimes D)$; the e is the random residual error, e~N(0, $V_E \otimes I$). V_A, V_D, and V_E are products of the 2x2 variance-covariance matrix defined by the correlation effects between pair-wise traits (r_A, r_D, r_E respectively) and the unique variance of each trait based on the CORGH variance structure in ASReml-R Ver. 3.0.

2.6.Genetic parameter estimates

We estimated the narrow-sense heritability of individual tree models for multiple environment analyses (supplementary materials) as follows,

$$\widehat{h^2_{ind}} = \frac{\widehat{\sigma^2_A}}{\widehat{\sigma^2_P}} = \frac{\widehat{\sigma^2_A}}{\left(\widehat{\sigma^2_A}+\widehat{\sigma^2_{ae}}+\widehat{\sigma^2_D}+\widehat{\sigma^2_{de}}+\widehat{\sigma^2_e}\right)} \quad (5)$$

$$\widehat{H^2_{ind}} = \frac{\widehat{\sigma^2_A}+\widehat{\sigma^2_D}}{\widehat{\sigma^2_P}} = \frac{\widehat{\sigma^2_A}+\widehat{\sigma^2_D}}{\left(\widehat{\sigma^2_A}+\widehat{\sigma^2_{ae}}+\widehat{\sigma^2_D}+\widehat{\sigma^2_{de}}+\widehat{\sigma^2_e}\right)} \quad (6)$$

where, $\widehat{\sigma^2_A}$ is the additive genetic variance component based on the individual tree model (1) and (4); $\widehat{\sigma^2_{ae}}$ is the additive genetic by site interaction variance component (GxE); $\widehat{\sigma^2_D}$ is the dominance genetic variance component; $\widehat{\sigma^2_{de}}$ is the dominance genetic by site interaction variance component; $\widehat{\sigma^2_e}$ is the residual environment variance for models with a simple variance; the among-trial average of residual variance is used for the heterogeneous residual model; $\widehat{\sigma^2_P}$ is the phenotypic variance component represented by the sum of $\widehat{\sigma^2_A}$, $\widehat{\sigma^2_{ae}}$, $\widehat{\sigma^2_D}$, $\widehat{\sigma^2_{de}}$, and $\widehat{\sigma^2_e}$.

Type-B additive genetic correlation was estimated as follows

$$\hat{r}_b = \frac{\widehat{\sigma_A^2}}{\left(\widehat{\sigma_A^2}+\widehat{\sigma_{ae}^2}\right)} (7)$$

where $\hat{r}_b$ is the type-B additive genetic correlation. The dominance genetic variance was not significantly different from zero and is not shown in the results. Only $\hat{r}_b$ was reported. The reliability of breeding value of half-sib parents was calculated as follows:

$$R_i = 1 - \frac{PEV}{\hat{\sigma}_i^2} = 1 - \frac{{se_i}^2}{\hat{\sigma}_A^2} (8)$$

where R_i is the reliability of the breeding value of the i-th parent, where PEV, prediction error variance, equals the standard error square of the predicted breeding value; and $\hat{\sigma}_A^2$ is the estimated additive genetic variance component.

We estimated the additive genetic (r_A) and phenotypic correlation (r_P) based on individual trees observations. The dominance genetic correlation was not significantly different from zero for trait pairs, so it was removed from the results. The additive genetic correlation between traits were directly given by the estimated parameter r_A from the multivariate model [4], so were the phenotypic correlations as follows,

$$r_P = \frac{r_A\sqrt{\hat{\sigma}_{A_i}\hat{\sigma}_{A_j}} + r_D\sqrt{\hat{\sigma}_{D_i}\hat{\sigma}_{D_j}} + r_E\sqrt{\hat{\sigma}_{E_i}\hat{\sigma}_{E_j}}}{\sqrt{(\hat{\sigma}_{A_i}+\hat{\sigma}_{D_i}+\hat{\sigma}_{E_i})(\hat{\sigma}_{A_j}+\hat{\sigma}_{D_j}+\hat{\sigma}_{E_j})}} (9)$$

$$r_G = \frac{r_A\sqrt{\hat{\sigma}_{A_i}\hat{\sigma}_{A_j}} + r_D\sqrt{\hat{\sigma}_{D_i}\hat{\sigma}_{D_j}}}{\sqrt{(\hat{\sigma}_{A_i}+\hat{\sigma}_{D_i})(\hat{\sigma}_{A_j}+\hat{\sigma}_{D_j})}} (10)$$

where $\hat{\sigma}_{A_i}$, $\hat{\sigma}_{D_i}$, and $\hat{\sigma}_{E_i}$ are the additive genetic, dominance genetic, residual variances estimate for trait i. All the significance of genetic correlations and variances were tested with likelihood between the full model versus the null model (assuming r_A=0 and r_D=0). The standard errors of variances and correlations were calculated with Delta method in ASReml-R Version 3.0. The total genetic correlation (r_G) was calculated though the numeric values are similar as r_A due to the low dominance genetic variances.

3. Results

3.1. Genetic parameters of multiple traits with univariate models

Multiple heritabilities were estimated including the individual tree narrow-sense (h^2_{ind}) and broad-sense heritability, as well as the half-sib (h^2_{HS}) and full-sib family heritability (h^2_{FS}) for height, DBH, basal area (BA), height increment from age 5 to 35 (HT_RC), green weight of stem-wood and -bark (WT) and volume of stem-wood and -bark (VOL), stem taper (TPR), and ice storm damage (D_ICE). Low to moderate family heritability was demonstrated for growth traits ranging from 0.1-0.4 across all the tests, while in the non-ice damage zone and only DBH and taper (TPR) had significant individual tree heritability ($\widehat{h^2_{ind}}$= 0.17 see Fig. 2). Height increment (HT_RC) showed the highest individual tree narrow-sense heritability in the non-ice damage zone ($\widehat{h^2_{ind}} = 0.38 \pm 0.08$) without significant non-additive genetic variance, while genetic control of the height increment was non-significant; therefore, no genetic gain can be estimated for height increment after the ice storm damage. For the ice damage zone, genetic control (e.g., $\widehat{h^2_{ind}}$) of DBH and TPR (related to DBH) were higher than other traits, with $\widehat{h^2_{ind}}$ of DBH and TRP reaching 0.2 and $\widehat{H^2_{ind}}$ of DBH and TPR reaching 0.35 and~0.4, respectively.

We found the additive genetic control is more discernable than dominance control. The individual broad-sense heritability ($\widehat{H^2_{ind}}$) ranged from 0 to 0.44 for growth, taper, and ice damage and was non-significant from zero except for DBH (0.32 ±0.10) in the ice storm damage zone. The ice damage trait showed low genetic control based on multiple heritability estimates in both zones with or without age and *post-hoc* adjustments. The family models used no complex *post-hoc* adjustments as the individual tree models. The broad-sense full-sib family mean heritability of ice damage was more than zero but still not significant (0.42 ± 0.32).

Type-B genetic correlation showed distinct values (Fig. 3.) between the narrow-sense genotype-by-environment effect GxE (rba, or $r_{B\text{-}A}$) based on the individual tree model and the estimates of the family model (RBAf, or $r_{B\text{-}A}$ with family models). The family model estimated higher GxE ($r_{B\text{-}A}$ =0.4-0.7 for growth) for both zones, while the individual tree model had non-significant GxE estimates especially for the ice damage zone. For $r_{B\text{-}A}$ of both family and individual tree models, DBH and height increment showed moderate to high GxE in the non-ice zone compared with other growth traits. Ice damage trait had inconsistent estimates of GxE for both models and among the two zones.

Akaike Information Criterion (AIC) and Bayesian Information Criterion (BIC) showed that the *post-hoc* adjustment improved model fitting for the univariate genetic parameter estimation. Yet the family model may have higher estimates of genetic parameters of growth traits, but less preferred model fitting due to the ignorance of micro-site spatial variations of the original RCBD design compared to the incomplete RCBD adjustments.

3.2. Genetic correlation and phenotypic correlations with the multivariate model

With the multivariate model, we found a genetic correlation as taller trees showed lower ice damage (-0.1 to -0.2, in Fig. 4. and Table 2). The direct correlation of breeding values of ice storm damage versus height reached -0.29 in the ice damage zone. However, in the non-ice damage zone, limited Pearson's correlation coefficients of breeding values were found among ice damage and height growth, while DBH was marginally related to the ice damage (r=0.11 in Fig. 5.). As expected, both genetic correlations and phenotypic correlations were found for growth traits. In the multivariate analyses, the pooled genetic correlation of ice damage for all trials was low for both height increment (-0.18*) and height (-0.11). Nonetheless, no significant phenotypic correlation was found for the ice damage trait. The incidental disturbance may alter the correlation between ice damage versus growth traits. The additive breeding value correlation in the ice damage zone indicates that taller trees at rotation tend to be resilient to ice damage, showing better capacity to recover from breakage. A potential synergy of ice tolerance and height growth is promising in this population. Height selection does not adversely affect tolerance to ice storms. No spatial *post-hoc* adjustment was used in the multivariate models, but the covariance between traits was employed. The genetic correlation calculated in separated zones is statistically non-estimable for multiple pairs of traits, so the pooled genetic correlation with more trials and total family variation was estimated (Table 2).

3.3. Potential response of ice tolerance under volume selection

Despite the global weak negative genetic correlation between ice damage and height increment or height growth or volume, volume improvement is still achievable when ice-damage infers additional selection pressure. To optimize simultaneous gains in productivity and ice damage resilience, we identified 'correlation breakers' among the parental population—elite genotypes that deviate from the trade-off between rapid volume growth and ice-damage susceptibility: Parental breeding values (BVs) for volume and ice-damage were evaluated via bi-variate scatter

plots (Fig. 6). The lower quadrant in red are the candidates for preferred ice damage tolerance (i.e., lower BVs depict increasing structural resilience) with height and volume genetic gains under 5%-40% selection ratio of families based on the breeding values. Since the correlation between the ranking and the breeding values of ice damage is not strong with a flat regression line (R^2<0.1), selecting the elite families for faster growth will not change the average of ice damage or tolerance as the opposite of the damage trait. The correlation breakers are the top performers with the lowest breeding values of ice damage with generate gain for both growth and tolerance to heavy icing. While height has historically served as a primary selection target, our heritability estimates for both height and volume collapsed to non-significance under ice-damaged conditions (Fig. 2; Appendix Table 4). This indicates that height-centric selection is unlikely to yield reliable genetic gains in such environments, as random environmental variance effectively masks underlying genetic variance that is not significantly different from zero.

4. Discussion

The influence of ice storms as a selection pressure becomes evident by comparing the changes of genetic parameters over two distinct environmental zones with different ice storm damage severity. In the zone without severe ice storm, genetic parameters such as additive genetic variance and heritability are higher than those in the zone with a severe ice storm. Extreme events such as ice storms with strong perturbations on stand structure can cause selection through differential impacts on fitness including outright mortality (Grant *et al. 2*017). However, episodic or random events are not an effective artificial selection tool because such selection pressure needs to be applied for multiple generations. One bottleneck for genetic trials and tree improvement is that typical breeding programs cannot afford multiple generations of losses of high-quality progeny tests, even though such experiments can provide informative data of family performance under such selection forces.

One difficulty in this study lies in precisely quantifying the genotype-by-environment (GxE) effect due to the lack of family-level replication across field sites. However, the seed source model projected moderate GxE in these long-running genetic trials. Tests involving ice damage subjected to physical injury showed no significant type-B genetic correlations suggesting either more balanced MET data are needed for improved GxE estimated or uncertain

GxE is projected here. More studies with finer defined ice damage scores and controlled experiments are needed for improved GxE characterization of ice damage. We tried a combined analysis of two environmental zones and noted declining significance potentially due to data unbalance during the later stage of the tests, e.g., after thinning and competition-induced mortality.

Our results showed that using the "correlation breakers" potentially improves both ice storm tolerance and growth plus stem taper over time. The "correlation breakers" usually represent family breeding values that deviate strongly from average in genetic correlation between traits that may have unfavorable genetic relationships (Klápště *et al. 2*022). Unlike a previous ice damage study in loblolly pine, we did not find a strong signal of the phenotypic correlation between height and ice damage (Aubrey *et al. 2*007). Our study did not reveal a specific trade-off between growth and ice tolerance; however, we observed a trend with respect to additive genetic correlation, where some taller trees exhibited greater tolerance to ice damage (r_A=-0.1, in that they recovered well with good height growth after being damaged by the severe ice storm). Although univariate BLUP models could not demonstrate the discernable heritability of ice damage recovery, our bivariate BLUP analysis demonstrated a moderate additive genetic correlation (r_A= -0.18) between growth and height recovery and a negligible genetic correlation (r_A= -0.1) between growth and tree height. Such correlation between growth and damage response to ice storms and frost stress can potentially yield promising selected families from the breeding populations when height and volume growth are traditionally the main objectives. We suggest that the average ice damage level will unlikely be altered by height selection due to the low additive genetic correlation. The correlation breakers in the top families will not compromise the ice storm tolerance of future generations in backward selections. These families can improve the seed orchard composition and future improvement of these populations. Both multivariate and univariate models (with *post-hoc* adjustment) agreed with the correlation between height growth and ice damage tolerance. The multivariate analyses could not remove all environmental heterogeneity and spatial noise, though the covariance estimates are robust.

The ice damage caused tree stem breakage at the leading meristem in an European study (Šēnhofa *et al. 2*020) and we found the same trend based on the genetic correlation and breeding value correlations. When trees are prone to have mechanical breakage of the stem, the tree height

will be inferior compared to the unbroken trees while the DBH of those trees might not necessarily be affected (Aubrey *et al. 2*007). Our results confirmed that the genetic control for DBH and taper were not negatively affected by ice storm damage although the actual tree height was certainly affected by storm damage. The frequency of experiencing stem breakage is low at the non-ice damage zone (4 trials) where the crooked growth pattern does not occur; however, overstory trees with higher DBH were significantly more vulnerable to mechanical damage during severe ice events based on a Norway spruce study (Šēnhofa *et al. 2*020). The social class of the trees may also be a factor of storm damage due to the thinning process and expansion of the radial growth of some tested trees in the same common garden experiments. While Šēnhofa *et al.*, (2020) observed lower damage in low-density, large-DBH stands, our study did not find the correlation at the individual tree level. Instead, our data indicate a negative relationship between height growth rate and ice-damage, suggesting that vigorous growth facilitates more effective physiological and morphological recovery after a storm. Visible storm damage (in this study) and the experimental stem breakage are not the exact same trait to be compared here, though the tree size and storm damage are genetically correlated. Additional controlled experiments are needed to provide multiple expressions and indicators of storm damage as well as recovery. In plantations, silviculture practices with different age classes and lower density can promote tree growth and sawlog quality at the older ages in other pioneering forest tree species (Kühn *et al. 2*021).

Moderate genetic control (0.1-0.4) for stem volume and taper, as well as ice storm tolerance will inform tree improvement and result in hardier plantations by allowing selection of "correlation breakers". Our previous study showed significant family heritability, which were also reported in this study. Our updated family models yielded substantially higher family-mean heritabilities for growth traits (~0.8–0.9±0.1–0.2 across trial zones), representing a ~10% increase over previous ANOVA-based estimates of full-sib family-mean heritability for DBH (Hossain et al. 2021). This improvement is largely driven by a reduction in residual error, which was achieved by fitting a heterogeneous variance-covariance structure in the current univariate models (Appendix A2). Even the improved residual variance structures and age adjustment of the family model without the *post-hoc* can improve the heritability estimates. Analytical techniques such as the *post-hoc* row-column adjustment can also be tested in additional non-model species with historically established trials. Non-additive genetic variance was not broadly

demonstrated in most of the traits assessed in this study though non-additive genetic effect of conifers has been reported as high as proportions (e.g., ~30%-100%) of the additive genetic variance (McKeand *et al. 2*008; Ivković *et al. 2*015; Berlin *et al. 2*019). We expect an improved design with more full-sib crosses or clones and single-tree plots to benefit the future estimates of the non-additive genetic variance (Ding *et al. 2*020). By selecting the families for the next breeding cycle, clonal tests could be established to evaluate both the dominance and epistasis genetic variances and potential gains for commercial and adaptational traits.

We estimated genetic correlations between semi-categorical ice damage scores and continuous growth traits using a multivariate linear mixed model (LMM) in ASReml. Although threshold generalized linear mixed models (GLMMs) are theoretically optimal for ordinal data (Weng et al. 2015; Gailis et al. 2020), fitting multivariate GLMMs across mixed data types and complex designs and pedigrees is computationally time-consuming and prone to convergence failure for this dataset. Consequently, treating ordinal scores as continuous variables remains a robust, standard approximation for estimating trait-trait genetic and phenotypic correlations (Weng et al. 2015; Gailis et al. 2020). This multiple linear mixed model framework (MLMM) ensured stable variance-covariance estimation, revealing an estimable genetic correlation between ice damage and growth.

For future tree improvement and seed zone design, we suggest multiple zones be constructed based on the projected ice storm or cold climate conditions. Principal component analysis of site means revealed separation between ice-damaged and non-damaged trials, with three Ozark-North trials clustering in the first quadrant and trial 32 (Ozark North) remaining distinct from the ice-damaged trials (Fig. 1). Ice storm damage was driven by geographic location and cold-temperature variables (e.g., latitude, longitude, EMT, MCMT), with basal area variation occurring independently of ice damage. The current zoning and provenance information can be used to guide such delineation of seed zones based on the long-term progeny of trial data. In addition, rapidly developing genomic tools for the southern pines (e.g., Tambarussi et al. 2025) can benefit the breeding programs by genotyping and identifying the genomic signals for selecting the “correlation breakers” as well as the family groups with high adaptability, resilience, and productivity for *in situ* reforestation and movement.

5. Conclusions

Our study used a series of long-term shortleaf pine progeny tests to demonstrate the potential of tree improvement for improving tree growth and stem taper traits in the face of an extreme ice storm that severely damaged some of the tests. Low to moderate heritability of growth rate and ice damage were reported based on 21,260 measured trees from 330 full-sib families, representing source populations and test locations in the Ouachita and adjacent Ozark Mountains of the US. We found that "correlation breakers" with respect to breeding values allow for genetic gain in both traits (e.g., height and volume). Tree improvement specialists can use these results for implementing directional selection of "correlation breakers" for both productivity and resilience gains in shortleaf pine as well as to better address the challenges posed by climate change and habitat degradation leading to improved populations for conserving threatened tree species and restoring degraded forest ecosystems.

Table captions

Table 1 Progeny test information and descriptive analyses of tree phenotypic measurement

Note, the ice damage (yes or no) from the severe ice storm event of December 2000 was recoded when the trees were measured in 2018 and 2019. The tree age (the measurement year minus the planting year) was nested within each trial, although most of the tests were measured at age 35. Sites 14, 28, 32, and 33 demonstrated no observable ice damage from the December 2000 storm. The family links show family connectivity between trials based on the hierarchical clustering with the Heatmap in R program.

Table 2 Estimates of additive genetic correlation among tested traits (upper diagonal), and phenotypic correlation (lower diagonal)

Note, Standard errors are in parentheses. HT_RC, height increment from age 5 to age 35; HT, tree height; DIA, DBH; CGWWB, complete tree green weight in kilograms of wood, and bark (kg); STRAIGHT, straightness; VL, tree volume (m^3); BA, basal area (m^2); D_ICE, ice damage; TAPER, "__", the estimate is rounded as 1.0 but the standard error is not estimable; *, p-value <0.05, the estimates were significantly different from zero. CGWWB and CCMWB were correlated with r>0.99 so only the CGWWB was reported in this table.

The upper diagonal was the additive genetic correlation; the lower diagonal was the phenotypic correlation. The standard errors were calculated with the delta method.

Figure captions

Fig. 1. Study area and trial locations in Arkansas in the context of the species range of *Pinus echinata*.

Note, a) The symbols of 15 USDA-FS progeny trial locations and natural species range of *P. echinata* in the USA with the extreme minimum temperature (EMT); b) The progeny tests and the five delineated zones based on the climate and geographical locations in Arkansas. The species range is based on the USDA-FS forest inventory data (Peters et al. 2019); the climate data were retrieved from the ClimateNA, http://climatena.ca/ (Wang et al. 2016).

Fig. 2. Narrow-sense heritability, broad-sense heritability, and family heritability of multiple traits in two zones (ice damage versus no-ice damage).

Note, Ice is zone with ice damage (11 trials); No-ice zone without ice damage (4 trials); h2(ind), narrow-sense heritability of individual tree model; H2b, broad-sense heritability of the individual tree model; h2R_f, narrow-sense heritability of the family model; h2BR_f, broad-sense heritability of the family model; h2HS, narrow-sense half-sib family mean heritability; h2FS, narrow-sense full-sib family mean heritability; h2bFS, broad-sense full-sib family heritability; h2w, narrow-sense within-family heritability; h2bw, broad-sense within-family heritability;

HT, height (m); DIA, DBH (cm); BA, basal area (m^2); HT_RC, height increment from age 5 to 35; CGWWB, complete tree green weight in kilograms of wood, and bark (kg); CCMWB, complete tree cubic meters of wood and bark (m^3); D_ICE, ice damage. Missing estimates are due to no convergence of the linear mixed model.

Fig. 3. Type-B genetic correlation of additive genetic effects of multiple traits at the ice damage zone (11 trials) versus no-ice damage zone (4 trials).

Note, HT, height (m); DIA, DBH (cm); HT_RC, height increment from age 5 to 35; CGWWB, complete tree green weight in kilograms of wood, and bark (kg); CCMWB, complete tree cubic meters of wood and bark (m^3); BA, basal area (m^2); D_ICE, ice damage. The first horizontal panel is the individual tree multivariate model (r_{bA}), while the second panel is based on the family multivariate model (R_{BAf}).

Fig. 4. Correlation and histogram of breeding values for multiple traits in the ice damage zone (11 trials).

Note, HT, height (m); DIA, DBH (cm); BA, basal area; HT_RC, height increment from age 5 to 35; CGWWB, complete tree green weight in kilograms of wood, and bark (kg); CCMWB, complete tree cubic meters of wood and bark (m^3); BA, basal area (m^2); D_ICE, ice damage. Pearson's correlation coefficients are in the right upper diagonal, the scatter plots are in the lower-left diagonal for the pairs of physiological variables, while the diagonal are the histograms of each variable. The *p*-values are denoted as following *** < 0.001, ** < 0.01, * < 0.05. HT_RC was only analyzed for the ice zone (11 trials) because the missing value was more than 25% (851/2961= 0.287).

Fig. 5. Pearson correlation, scatter plot and histogram of breeding values for multiple traits in the no ice damage zone (4 trials).

Note, HT, height (m); DIA, DBH (cm); BA, basal area; HT_RC, height increment from age 5 to 35; CGWWB, complete tree green weight in kilograms of wood, and bark (kg); CCMWB, complete tree cubic meters of wood and bark (m^3); BA, basal area (m^2); D_ICE, ice damage. Pearson's correlation coefficients are in the right upper diagonal, the scatter plots are in the lower-left diagonal for the pairs of physiological variables, while the diagonal are the histograms of each variable. The p-values are denoted as following *** < 0.001, ** < 0.01, * < 0.05.

Fig. 6. Scatter plot of height ranking and the breeding values of ice damage at the no ice zone (4 trials) and the ice damage zone (11 trials).

Note, the orange color depicts the top ranked families of volume growth (60 percentiles to 80 percentiles); the green color illustrates the top ranked families from 80 percentiles to 90

percentiles; the blue color shows the families from 90 percentiles to 95 percentiles; the red color depicts the top families above 95 percentiles. The red rectangle captures the candidate's families with both genetic gains in growth and frost damage tolerance.

Acknowledgement

We thank the following for invaluable assistance over the course of this work: Carolyn Pike (USDA Forest Service, Eastern Region, State, Private and Tribal Forestry) for organizing the rotation-aged measurement data for initial analyses; Ben Rowland (USDA Forest Service, Southern Region) for providing information on earlier measurements of these progeny tests; Virginia McDaniel (USDA Forest Service, Southern Research Station) for field data collection and reconstruction of the X,Y tree-coordinates within the progeny tests; Ben Bartlett (formerly Texas A&M Forest Service, Western Gulf Forest Tree improvement Program) for helping to organize the data set for quantitative genetic analyses; and John Blanton (retired USDA Forest Service, Southern Region) for surveying and assessing the potential for re-measuring these progeny tests.

In memoriam of our late co-author Dr. Don C. Bragg, the honorable and distinguished silviculture scientist of southern pines and great leader in the forestry community.

Funding Statement:

This work was supported in part by the United States Department of Agriculture (USDA) Forest Service through the Shortleaf Pine Breeding Program, and the USDA Forest Service grant (FS-24-JV-11111137-115) to CD and HC; the Texas A&M Forest Service Western Gulf Forest Tree Improvement Program; the Schatz Colloquium for Tree Genetics, which provided a graduate grant to CD; the Alabama Agricultural Experiment Station, Auburn University, through the AgR-Seed program to CD; and the USDA National Institute of Food and Agriculture (NIFA), Agriculture and Food Research Initiative (AFRI) C1701 grant to HC and CD.

Data Archiving Statement:

The individual-tree phenotypic dataset, pedigree file from the 15 progeny trials analyzed in this study have been deposited in Zenodo (https://doi.org/10.5281/zenodo.20417278). The deposit includes tree-level measurements of survival, height, DBH, basal area, volume, ice-storm damage, health, and stem straightness. Data will be publicly released upon publication.

Author contributions

Chen Ding: Conceptualization, Data curation, Formal analysis, Writing – original draft, Writing – review & editing. **Shaik M. Hossain:** Conceptualization, Data curation, Writing – review & editing. **Yuhui Weng:** Data analysis, Writing – review & editing. **Hao Chen:** Data analysis, Writing – review & editing. **Barbara S. Crane**: Writing – procured the funding for Blanton's surveys & assessments, review & editing. **Earl M. Raley**: Data curation, Conceptualization, Data analysis, Writing – review & editing, Funding acquisition. **Don C. Bragg**: Conceptualization, Writing – original draft, Writing – review & editing, Project administration. **C. Dana Nelson:** Conceptualization, Data curation, Writing – original draft, Writing – review & editing, Project administration, Funding acquisition.

Conflict of interest

The authors have no conflict of interests.

Plant-Studies compliance statement

All progeny trials were established and maintained by the USDA Forest Service under standard agency authority; no additional permits were required. The work complies with institutional, national, and international guidelines applicable to research plants.

References

Aitken, S.N., Bemmels, J.B., 2016. Time to get moving: assisted gene flow of forest trees. Evolutionary Applications 9, 271-290.

Aitken, S.N., Yeaman, S., Holliday, J.A., Wang, T., Curtis-McLane, S., 2008. Adaptation, migration or extirpation: climate change outcomes for tree populations. Evolutionary Applications 1, 95-111.

Alberto, F.J., Aitken, S.N., Alia, R., Gonzalez-Martinez, S.C., Hanninen, H., Kremer, A., Lefevre, F., Lenormand, T., Yeaman, S., Whetten, R., Savolainen, O., 2013. Potential for evolutionary responses to climate change - evidence from tree populations. Global Change Biology 19, 1645-1661.

Anderegg, W.R., Plavcova, L., Anderegg, L.D., Hacke, U.G., Berry, J.A., Field, C.B., 2013. Drought's legacy: multiyear hydraulic deterioration underlies widespread aspen forest die-off and portends increased future risk. Global Change Biology 19, 1188-1196.

Anderegg, W.R.L., Hicke, J.A., Fisher, R.A., Allen, C.D., Aukema, J., Bentz, B., Hood, S., Lichstein, J.W., Macalady, A.K., McDowell, N., Pan, Y.D., Raffa, K., Sala, A., Shaw, J.D., Stephenson, N.L.,

708 Tague, C., Zeppel, M., 2015. Tree mortality from drought, insects, and their interactions in a changing
709 climate. New Phytologist 208, 674-683.

710 Arora, R., Taulavuori, K., 2016. Increased Risk of Freeze Damage in Woody Perennials VIS-À-VIS
711 Climate Change: Importance of Deacclimation and Dormancy Response. Frontiers in Environmental
712 Science 4.

713 Aubrey, D.P., Coleman, M.D., Coyle, D.R., 2007. Ice Damage in Loblolly Pine: Understanding the
714 Factors That Influence Susceptibility. Forest Science 53, 580-589.

715 Baltunis, B.S., Huber, D.A., White, T.L., Goldfarb, B., Stelzer, H.E., 2005. Genetic effects of rooting
716 loblolly pine stem cuttings from a partial diallel mating design. Canadian Journal of Forest Research 35,
717 1098-1108.

718 Berlin, M., Jansson, G., Högberg, K.-A., Helmersson, A., 2019. Analysis of non-additive genetic effects
719 in Norway spruce. Tree Genetics & Genomes 15, 42.

720 Bian, L.M., Zheng, R.H., Su, S.D., Lin, H.Z., Xiao, H., Wu, H.X., Shi, J.S., 2017. Spatial analysis
721 increases efficiency of progeny testing of Chinese fir. Journal of Forestry Research 28, 445-452.

722 Coble, D.W., Lee, Y.-J., Lenhart, J.D., 2004. Project Report No. 66, Metric Volume and Biomass
723 Prediction Equations for Loblolly and Slash Pine Trees Planted in Unmanaged Pine Plantations in East
724 Texas Informal Project Reports. 4. Stephen F. Austin State University, TX.
725 https://scholarworks.sfasu.edu/etpprp_project_reports/4.

726 De Faveri, J., Verbyla, A.P., Cullis, B.R., Pitchford, W.S., Thompson, R., 2017. Residual Variance–
727 Covariance Modelling in Analysis of Multivariate Data from Variety Selection Trials. Journal of
728 Agricultural, Biological, and Environmental Statistics 22, 1-22.

729 Ding, C., Brouard, J.S., 2022. Assisted migration is plausible for a boreal tree species under climate
730 change: a quantitative and population genetics study of trembling aspen (*Populus tremuloides* Michx.) in
731 western Canada. Ecology and Evolution (Accepted).

732 Ding, C., Hamann, A., Yang, R.C., Brouard, J.S., 2020. Genetic parameters of growth and adaptive traits
733 in aspen (*Populus tremuloides*): Implications for tree breeding in a warming world. PLoS One 15,
734 e0229225.

735 Ding, C., Weng, Y., Byram, T.D., Bartlett, B.D., Raley, E.M., 2023. Post hoc experimental designs
736 improve genetic trial analyses: A case study of cherrybark oak (*Quercus pagoda* Raf.) genetic evaluation
737 in the western Gulf region, USA. PLoS One 18, e0285150.

738 Dong, L., Xie, Y., Sun, X., 2019. Full-diallel-based analysis of genetic parameters for growth traits in
739 Japanese larch (*Larix kaempferi*). New Forests 51, 261-271.

740 Gailis, A., Zeltiņš, P., Purviņa, D., et al., 2020. Genetic parameters of growth and quality traits in
741 open-pollinated silver birch progeny tests. *Silva Fennica*, 54(3), 10220.

Gezan, S.A., Huber, D.A., White, T.L., 2006a. Post hoc blocking to improve heritability and precision of best linear unbiased genetic predictions. Canadian Journal of Forest Research 36, 2141-2147.

Gezan, S.A., White, T.L., Huber, D.A., 2006b. Comparison of experimental designs for clonal forestry using simulated data. Forest Science 52, 108-116.

Grant, P.R., Grant, B.R., Huey, R.B., Johnson, M.T.J., Knoll, A.H., Schmitt, J., 2017. Evolution caused by extreme events. Philosophical Transactions of the Royal Society B: Biological Sciences 372.

Hossain, S.M., Bragg, D.C., McDaniel, V.L., Pike, C.C., Crane, B.S., Nelson, C.D., 2021. Evaluation of Long-Term Shortleaf Pine Progeny Tests in the Ouachita and Ozark National Forests, USA. Forests 12, 953.

Hu, Y., Guy, R.D., Soolanayakanahally, R.Y., 2022. Genotypic variation in C and N isotope discrimination suggests local adaptation of heart-leaved willow. Tree Physiology 42, 32-43.

Intergovernmental Panel on Climate Change, 2023. Summary for Policymakers. In: Intergovernmental Panel on Climate Change (Ed.), Climate Change 2022 – Impacts, Adaptation and Vulnerability: Working Group II Contribution to the Sixth Assessment Report of the Intergovernmental Panel on Climate Change. Cambridge University Press, Cambridge, pp. 3-34.

Isabel, N., Holliday, J.A., Aitken, S.N., 2020. Forest genomics: Advancing climate adaptation, forest health, productivity, and conservation. Evolutionary Applications 13, 3-10.

Isik, F., Holland, J., Maltecca, C., 2017. Genetic Data Analysis for Plant and Animal Breeding. Springer International Publishing, Cham, Switzerland.

Ivković, M., Gapare, W., Yang, H., Dutkowski, G., Buxton, P., Wu, H., 2015. Pattern of genotype by environment interaction for radiata pine in southern Australia. Annals of Forest Science 72, 391-401.

Jansson, G., Li, B., 2004a. Genetic gains of full-sib families from disconnected diallels in loblolly pine. Silvae Genetica 53, 60-64.

Jansson, G., Li, B., 2004b. Genetic gains of full-sib families from disconnected diallels in loblolly pine. Silvae Genetica 53, 60-64.

Katrevics, J., Miezite, O., Luguza, S., Straupe, I., Jansone, B., 2020. Stem Defects in Low-Density Norway Spruce Plantations in Hemiboreal Forests. International Multidisciplinary Scientific GeoConference: SGEM 20, 715-722.

Keller, S.R., Soolanayakanahally, R.Y., Guy, R.D., Silim, S.N., Olson, M.S., Tiffin, P., 2011. Climate-driven local adaptation of ecophysiology and phenology in balsam poplar, *Populus balsamifera* L. (Salicaceae). American Journal of Botany 98, 99-108.

Klápště, J., Telfer, E.J., Dungey, H.S., Graham, N.J., 2022. Chasing genetic correlation breakers to stimulate population resilience to climate change. Scientific Reports 12, 8238.

Klopčič, M., Poljanec, A., Dolinar, M., Kastelec, D., Bončina, A., 2019. Ice-storm damage to trees in mixed Central European forests: damage patterns, predictors and susceptibility of tree species. Forestry: An International Journal of Forest Research 93, 430-443.

Kühn, H., Loguercio, G.A., Caselli, M., Thren, M., 2021. Growth and Potential of Lomatia hirsuta Forests from Stump Shoots in the Valley of El Manso/Patagonia/Argentina. Forests 12, 923.

Leuschner, C., Weithmann, G., Bat-Enerel, B., Weigel, R., 2023. The Future of European Beech in Northern Germany—Climate Change Vulnerability and Adaptation Potential. Forests 14, 1448.

Li, Z., Gao, C., Li, J., Wang, L., Cui, K., 2024. Variation in growth traits and early evaluation of the selection of intra and interspecific hybrid progeny of *Pinus yunnanensis*. New Forests 56, 14.

McKeand, S.E., Li, B., Grissom, J., Isik, F., Jayawickrama, K., 2008. Genetic parameter estimates for growth traits from diallel tests of loblolly pine throughout the southeastern United States. Silvae Genetica 57, 101-110.

Montwe, D., Isaac-Renton, M., Hamann, A., Spiecker, H., 2018. Cold adaptation recorded in tree rings highlights risks associated with climate change and assisted migration. Nature Communications 9, 1574.

Peters, M.P., Iverson, L.R., Prasad, A.M., Matthews, S.N., 2019. Utilizing the density of inventory samples to define a hybrid lattice for species distribution models: DISTRIB-II for 135 eastern U.S. trees. Ecology and Evolution 9, 8876-8899.

PRISM Climate Group, 2013. 30-yr Normal Mean Temperature [Map]: Annual (Period: 1981–2010). Oregon State University, Corvallis, OR, USA. http://www.prism.oregonstate.edu/normals/.

Pugh, A.L., Westerman, D.A., 2014. Mean annual, seasonal, and monthly precipitation and runoff in Arkansas, 1951-2011. USGS Scientific Investigations Report 5006, 40.

Rehfeldt, G.E., Ying, C.C., Spittlehouse, D.L., Hamilton, D.A., 1999. Genetic responses to climate in *Pinus contorta*: Niche breadth, climate change, and reforestation. Ecological Monographs 69, 375-407.

Rustad, L.E., Campbell, J.L., Driscoll, C.T., Fahey, T.J., Groffman, P.M., Schaberg, P.G., Hawley, G.J., Halm, I., Bowles, F., Leuenberger, W., Schwaner, G., Winant, G., Leonardi, B., 2020. Experimental approach and initial forest response to a simulated ice storm experiment in a northern hardwood forest. PLoS One 15, e0239619.

Šēnhofa, S., Katrevičs, J., Adamovičs, A., Bičkovskis, K., Bāders, E., Donis, J., Jansons, Ā., 2020. Tree Damage by Ice Accumulation in Norway Spruce (*Picea abies* (L.) Karst.) Stands Regarding Stand Characteristics. Forests 11, 679.

Shalizi, M.N., 2020. Genetic Parameter Estimates and Prediction of Genetic Merit in Clonal Populations of *Pinus taeda* L. Using Expected and Realized Genomic Relationships. North Carolina State University, United States, p. 234.

Shalizi, M.N., Isik, F., 2019. Genetic parameter estimates and GxE interaction in a large cloned population of *Pinus taeda* L. Tree Genetics & Genomes 15, 46.

Stewart, J.F., Will, R.E., Crane, B.S., Nelson, C.D., 2016. The genetics of shortleaf pine (*Pinus echinata* Mill.) with implications for restoration and management. Tree Genetics & Genomes 12, 98.

Szmyt, J., Dering, M., 2024. Adaptive Silviculture and Climate Change—A Forced Marriage of the 21st Century? Sustainability 16, 2703.

Tambarussi, E.V., Shalizi, M.N., Grattapaglia, D., Hodge, G., Isik, F., Paludeto, J.G.Z., et al., 2025. Genome-wide SNP-based relationships improve genetic parameter estimates and genomic prediction of growth traits in a large operational breeding trials of *Pinus taeda* L. Forestry: An International Journal of Forest Research 98(5), 692-705.

Tiarks, A.E., Baldwin JR, C., 1999. Validation of volume and taper equations for loblolly, shortleaf and slash pine. In: Proceeding of Tenth Biennial Southern Silvicultural Research Conference, Shreveport, LA, February 16–17. US Forest Service General Technical Report SRS-30, Asheville, NC, pp. 497-500.

Tyrmi, J.S., Vuosku, J., Acosta, J.J., Li, Z., Sterck, L., Cervera, M.T., Savolainen, O., Pyhäjärvi, T., 2020. Genomics of Clinal Local Adaptation in *Pinus sylvestris* Under Continuous Environmental and Spatial Genetic Setting. G3 (Bethesda, Md.) 10, 2683-2696.

Wang, L., Tiffin, P., Olson, M.S., 2014. Timing for success: expression phenotype and local adaptation related to latitude in the boreal forest tree, *Populus balsamifera*. Tree Genetics & Genomes 10, 911-922.

Wang, T., Hamann, A., Spittlehouse, D., Carroll, C., 2016. Locally Downscaled and Spatially Customizable Climate Data for Historical and Future Periods for North America. PLoS One 11, e0156720.

Ware, I.M., Van Nuland, M.E., Yang, Z.K., Schadt, C.W., Schweitzer, J.A., Bailey, J.K., 2021. Climate-driven divergence in plant-microbiome interactions generates range-wide variation in bud break phenology. Communications Biology 4, 748.

Weng, Y.H., Tosh, K., Park, Y.S., Fullarton, M.S., 2015. Genetic parameters of growth and stem quality traits for jack pine second-generation progeny tested in New Brunswick. Canadian Journal of Forest Research, 45(9), 1265-1272.

FAO, 2025. Global Forest Resources Assessment 2025. https://doi.org/10.4060/cd6709en

Woods, A., Foti, T., Chapman, S., Omernik, J., Wise, J., Murray, E., Prior, W., Pagan, J., Comstock, J., Radford, M., 2004. Ecoregions of Arkansas (color poster with map, descriptive text, summary tables, and photographs). US Geological Survey map scale 1.

Worrall, J.J., Rehfeldt, G.E., Hamann, A., Hogg, E.H., Marchetti, S.B., Michaelian, M., Gray, L.K., 2013. Recent declines of *Populus tremuloides* in North America linked to climate. Forest Ecology and Management 299, 35-51.

Wu, H., Matheson, A.C., 2001. Analyses of half-diallel mating designs with missing crosses: Theory and SAS program for testing and estimating GCA and SCA variance components. Silvae Genetica 50, 265-271.

Wuebbles, D., Meehl, G., Hayhoe, K., Karl, T.R., Kunkel, K., Santer, B., Wehner, M., Colle, B., Fischer, E.M., Fu, R., 2014. CMIP5 climate model analyses: climate extremes in the United States. Bulletin of the American Meteorological Society 95, 571-583.

Xiang, B., Li, B., Isik, F., 2003a. Time trend of genetic parameters in growth traits of *Pinus taeda* L. Silvae Genetica 52, 114-120.

Xing, L., Gezan, S., Kenworthy, K., Unruh, J.B., Munoz, P., 2017. Improved genetic parameter estimations in zoysiagrass by implementing post hoc blocking. Euphytica 213, 195.

Ye, Z., O'Neill, G.A., Wang, T., 2023. Optimization and validation of universal response functions for interior spruce (*Picea glauca*, *Picea engelmannii*, and their hybrids). Forest Ecology and Management 550, 121509.

Zhang, J., Peter, G.F., Powell, G.L., White, T.L., Gezan, S.A., 2015. Comparison of breeding values estimated between single-tree and multiple-tree plots for a slash pine population. Tree Genetics & Genomes 11, 48.

Zhang, M., Suren, H., Holliday, J.A., 2019. Phenotypic and Genomic Local Adaptation across Latitude and Altitude in *Populus trichocarpa*. Genome Biology and Evolution 11, 2256-2272.

Tables

Table 1 Progeny test site information and descriptive analyses of tree phenotypic measurement.

Site	Geographic Zone	Family -links	Year	Lat	Long	Female #	Male #	Family #	Design Rep	Tree #	Age	Planted Year	Height (m)	DBH (cm)	Volume (m^3)	Ice damage%
1	Ouachita - East (South)	e	1978	34.548	-93.600	15	22	25	4	910	40	1978	19.44	23.97	1.37	38.5
31	Ouachita - East (South)	c	1985	34.486	-93.505	13	15	29	5	1310	33	1985	19.61	26.71	0.98	65.3
5	Ouachita - East (South)	f	1981	34.579	-93.879	15	17	36	4	1350	38	1981	17.38	23.31	1.06	75.7
21	Ouachita - East (Central)	e	1984	34.757	-93.642	14	15	35	4	1340	34	1984	18.21	25.07	0.90	88.8
29	Ouachita - East (Central)	f	1985	34.772	-93.743	15	16	30	5	1310	33	1985	15.90	22.82	0.61	65.9
48	Ouachita - East (Central)	f	1987	34.802	-93.671	14	15	31	5	1480	31	1987	16.64	24.84	0.60	88.3
19	Ouachita - East (South)	a	1984	34.462	-93.858	15	16	35	5	1720	34	1984	20.92	28.56	1.26	76.1
25	Ouachita - West (Central)	d	1984	34.872	-93.976	16	16	37	5	1700	35	1984	17.40	22.49	0.74	68.9
6	Ouachita - West (Central)	a	1981	34.735	-94.191	17	16	37	5	1600	38	1981	15.81	23.02	0.91	93.3
10	Ouachita - West (South)	c	1982	34.573	-94.423	15	16	35	4	1360	37	1982	15.36	19.66	0.61	34.2
38	Ouachita - West (South)	b	1986	34.386	-94.217	14	16	28	5	1210	33	1986	20.95	26.86	1.09	36.9
14	Ozark - North	b	1984	35.444	-92.846	15	16	33	5	1600	35	1984	19.24	23.88	0.95	8.0
28	Ozark - North	d	1987	35.640	-93.923	20	21	34	5	1600	32	1987	20.62	25.31	0.86	8.8
32	Ozark - North	f	1988	35.698	-93.345	17	17	37	3	1080	31	1988	19.62	24.35	0.66	2.2
33	Ozark - North	e	1988	35.186	-93.450	17	20	34	5	1690	31	1988	20.24	24.14	0.73	4.1
Total						126	125	330	69	21260			18.49	24.33	0.89	50.3

Note, Ice damage from December 2000 storm was inferred during the re-measurement in 2018 and 2019 by the characteristic stem deformity. Tree ages are shown during the re-measurements made in 2018 and 2019. The sites 14, 28, 32, and 33 demonstrated essentially no ice damage. The family links show family connectivity between trials based on the hierarchical clustering with the Heatmap in R program. The more similar the letters the tighter link between the tested families (connectivity).

Table 2 Overall site estimates of additive genetic correlation among tested traits (upper diagonal), and phenotypic correlation (lower diagonal). Standard errors are in parentheses.

	HT_RC	HT	DIA	WT	VOL	BA	D_ICE	TPR
HT_RC	--	--	**0.728 (0.056) ***	**0.927 (0.039) ***	**0.942 (0.035) ***	**0.705 (0.055) ***	**-0.181 (0.047) ***	**0.785 (0.053) ***
HT	**0.075 (0.015) ***	--	**0.776 (0.040) ***	**0.953 (0.026) ***	**0.963 (0.023) ***	**0.748 (0.041) ***	**-0.114 (0.035) ***	**0.831 (0.038) ***
DIA	-0.006 (0.022)	-0.006 (0.018)	--	--	--	--	-0.060 (0.038)	--
WT	-0.007 (0.018)	-0.006 (0.014)	**0.133 (0.013) ***	--	--	--	**-0.090 (0.039) ***	--
VOL	-0.007 (0.017)	-0.005 (0.014)	**0.130 (0.013) ***	**0.576 (0.007) ***	--	--	**-0.093 (0.039) ***	--
BA	-0.006 (0.022)	-0.006 (0.019)	**0.154 (0.013) ***	**0.138 (0.013) ***	**0.135 (0.013) ***	--	-0.063 (0.038)	--
D_ICE	-0.002 (0.024)	-0.002 (0.020)	-0.001 (0.018)	-0.001 (0.019)	-0.001 (0.019)	-0.001 (0.019)	--	-0.064 (0.038)
TPR	-0.007 (0.021)	-0.006 (0.017)	**0.158 (0.013) ***	**0.134 (0.013) ***	**0.131 (0.013) ***	0.152 (0.013) *	-0.002 (0.018)	--

Note, HT_RC, height increment from age 5 to age 35; HT, tree height (m); DBH stem diameter at breast height; WT, green weight stem wood and bark (kg); VOL, stem volume (m^3); BA, basal area (m^2); D_ICE, ice damage; TPR, stem taper; the diagonal are the correlation as one which are not presented; "--" in the upper and lower panels denote that estimate is rounded as 1.0 but the standard error is not estimable; *, p-value <0.05, the estimates were significantly different from zero. WT and VOL were correlated with r>0.99 so only the WT is reported in the table.

The upper diagonal is the additive genetic correlations; the lower diagonal is the phenotypic correlations. The standard errors were calculated with the delta method.

Figures

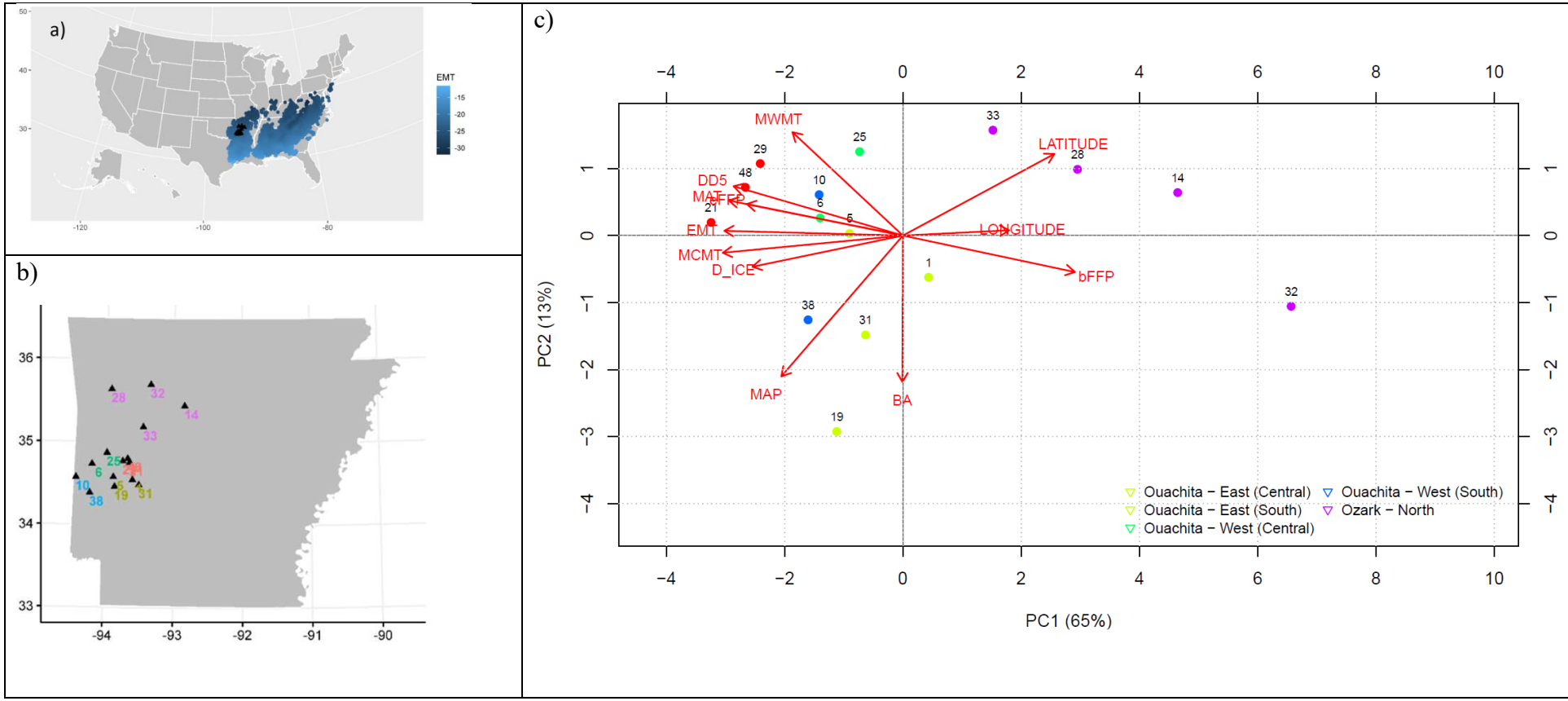

Fig. 1. Study area and trial locations in Arkansas in the context of the species range of shortleaf pine with x-axis as the longitude, and the y-axis as the latitude as well as the PCA of site climate and the basal area per acre.

Panels: a) The symbols of 15 USDA-FS progeny trial locations and natural species range of shortleaf pine in the USA with the extreme minimum temperature (EMT); b) The progeny tests locations and the five delineated zones based on the climate and geographical locations in Arkansas; c) Principal component analysis (PCA) of site climate and the basal area per acre.

Note, Each triangle represents the trial locations while the color represents the zones of trial (Table 1). Trial numbers are listed in Table 1. The circle of a) de Families with both ice storm tolerance and Families with both ice storm tolerance and picts the centroid location of trials together in Arkansas. The species range is based on the USDA-FS forest inventory data (Peters *et al.*, 2019); the climate data were retrieved from the ClimateNA, http://climatena.ca/ (Wang *et al.*, 2016). The climate data were retrieved from the ClimateNA

889 (http://climatena.ca/, (Wang *et al.*, 2016). The climatic variables include MAT, Mean annual temperature (°C); MAP, mean annual
890 precipitation (mm); MWMT, mean warmest month temperature (°C); MCMT, mean coolest month temperature (°C); EMT, extreme
891 minimum temperature over 30 years (°C); DD5, degree-days above 5°C; bFFP, date-of-year as the beginning of frost free period;
892 eFFP, date-of-year as the end of frost free period. D_ICE, ice damage trait; BA, average tree basal area; HT, average tree height of last
893 measurement (m); DIA, average DBH of last measurement (cm).

894 In c) Four Ouachita trials (1, 6, 11, and 14) are grouped in one cluster; all four Ozark trials are grouped in a second cluster; the rest of
895 the Ouachita trials are grouped in the third cluster. The zones of trials were depicted in colors in the legend respectively. Principal
896 Component 1 (PC1) indicated geographic and climate distance index i.e., latitude, longitude, and extreme minimum temperature
897 (EMT) and other climatic variable distances (not equal to geographical distances), which accounted for 65% of the total variance. PC2
898 indicated basal area growth of each site which is not linked to the climatic variables of trials except the mean annual precipitation. Ice
899 damage is associated with the longitude, extreme minimum temperature (EMT), and the min temperature of the coldest month
900 (MCMT). The grouping colors of seed zones are Ouachita-East (red), Ouachita-West (blue), Ouachita-East (South)(yellow), Ozark-
901 North (purple), and Ouachita -West (light green).

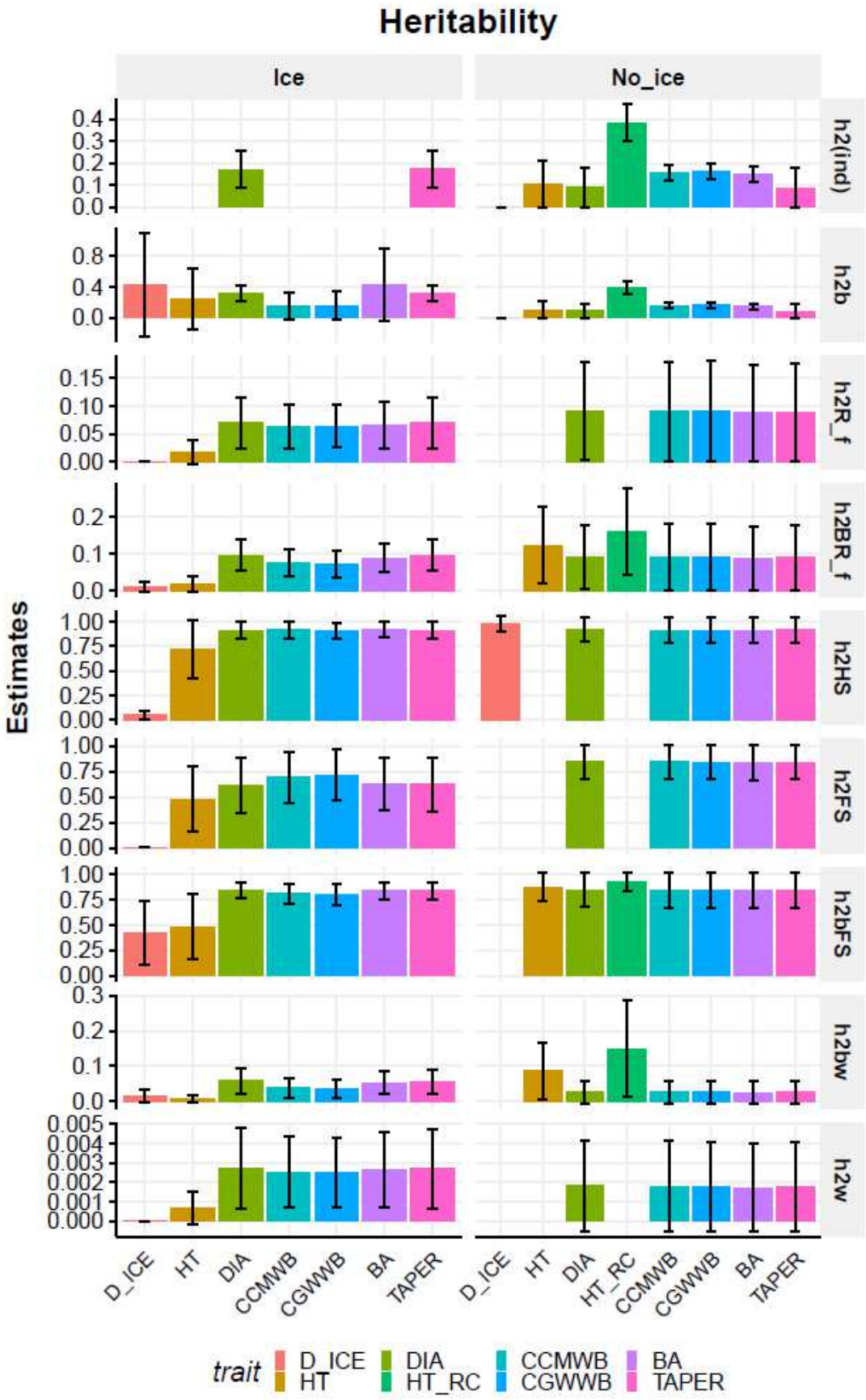
Heritability
Ice
No_ice
h2(ind)
h2b
h2R_f
h2BR_f
h2HS
h2FS
h2bFS
h2bw
h2w
Estimates
D_ICE
HT
DIA
HT_RC
CCMWB
CGWWB
BA
TAPER
trait

Fig. 2. Narrow-sense heritability, broad-sense heritability, and family heritability of multiple traits at two zones (ice damage versus non-ice).

Note, Ice is zone with ice damage (11 trials); Non-ice zone without ice damage; h2(ind), narrow-sense heritability of individual tree model; H2b, broad-sense heritability of the individual tree model; h2R_f, narrow-sense heritability of the family model; h2BR_f, broad-sense heritability of the family model; h2HS, narrow-sense half-sib family mean heritability; h2FS, narrow-sense full-sib family mean heritability; h2bFS, broad-sense full-sib family heritability; h2w, narrow-sense within-family heritability; h2bw, broad-sense within-family heritability;

HT, height (m); DIA, DBH (cm); BA, basal area (m^2); HT_RC, height increment from age 5 to 35; CGWWB, complete tree green weight in kilograms of wood, and bark (kg); CCMWB, complete tree cubic meters of wood and bark (m^3); D_ICE, ice damage. Missing estimates are due to no convergence of the linear mixed model.

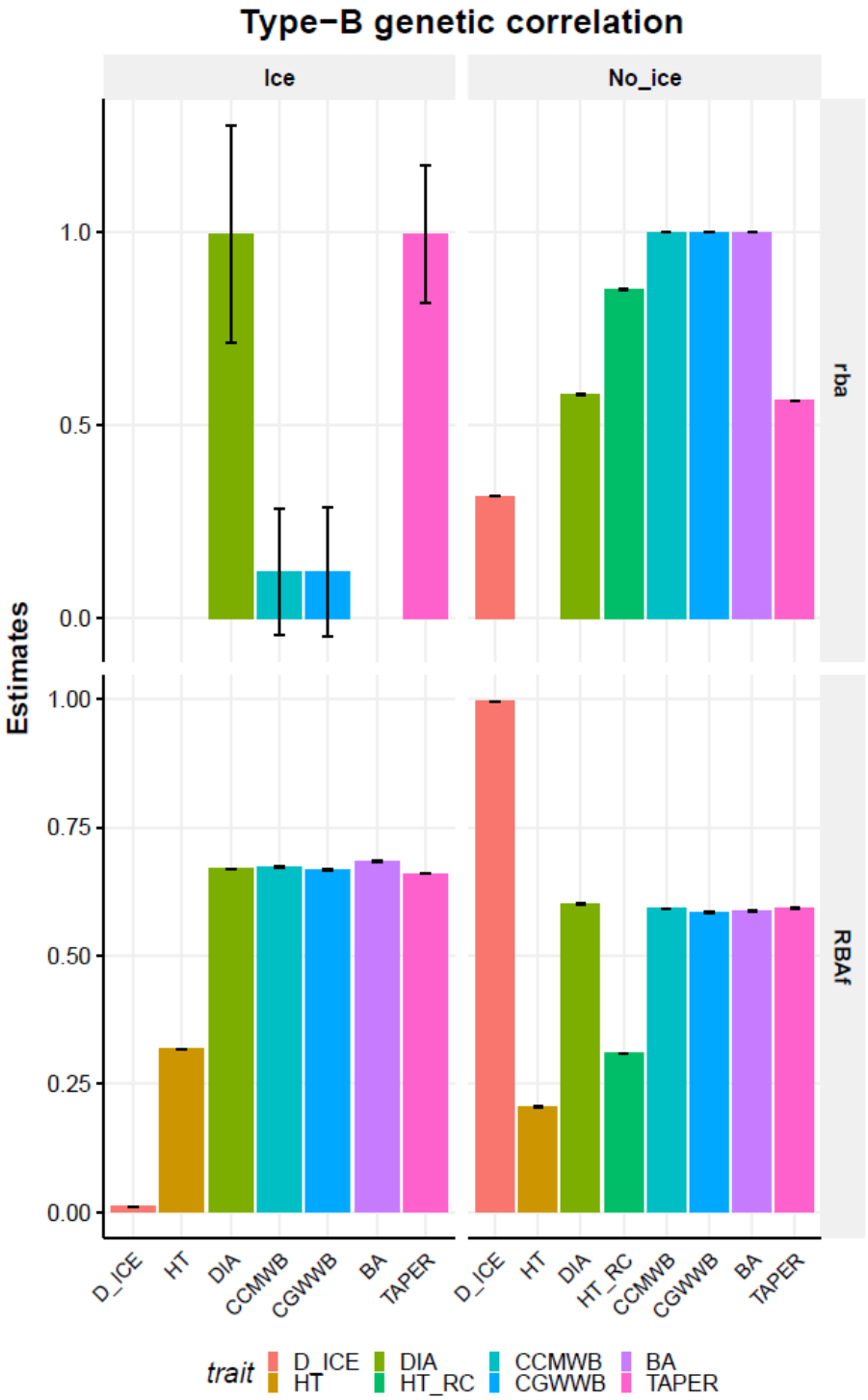

916

917 **Fig. 3.** Type-B genetic correlation of additive genetic effects of multiple traits at the ice damage
918 zone (11 trials) versus no-ice damage zone (4 trials).

919 Note, HT, height (m); DIA, DBH (cm); HT_RC, height increment from age 5 to 35; CGWWB,
920 complete tree green weight in kilograms of wood, and bark (kg); CCMWB, complete tree cubic

meters of wood and bark (m^3); BA, basal area (m^2); D_ICE, ice damage. The first horizontal panel is the individual tree multivariate model (r_{bA}), while the second panel is based on the family multivariate model (R_{BAf}).

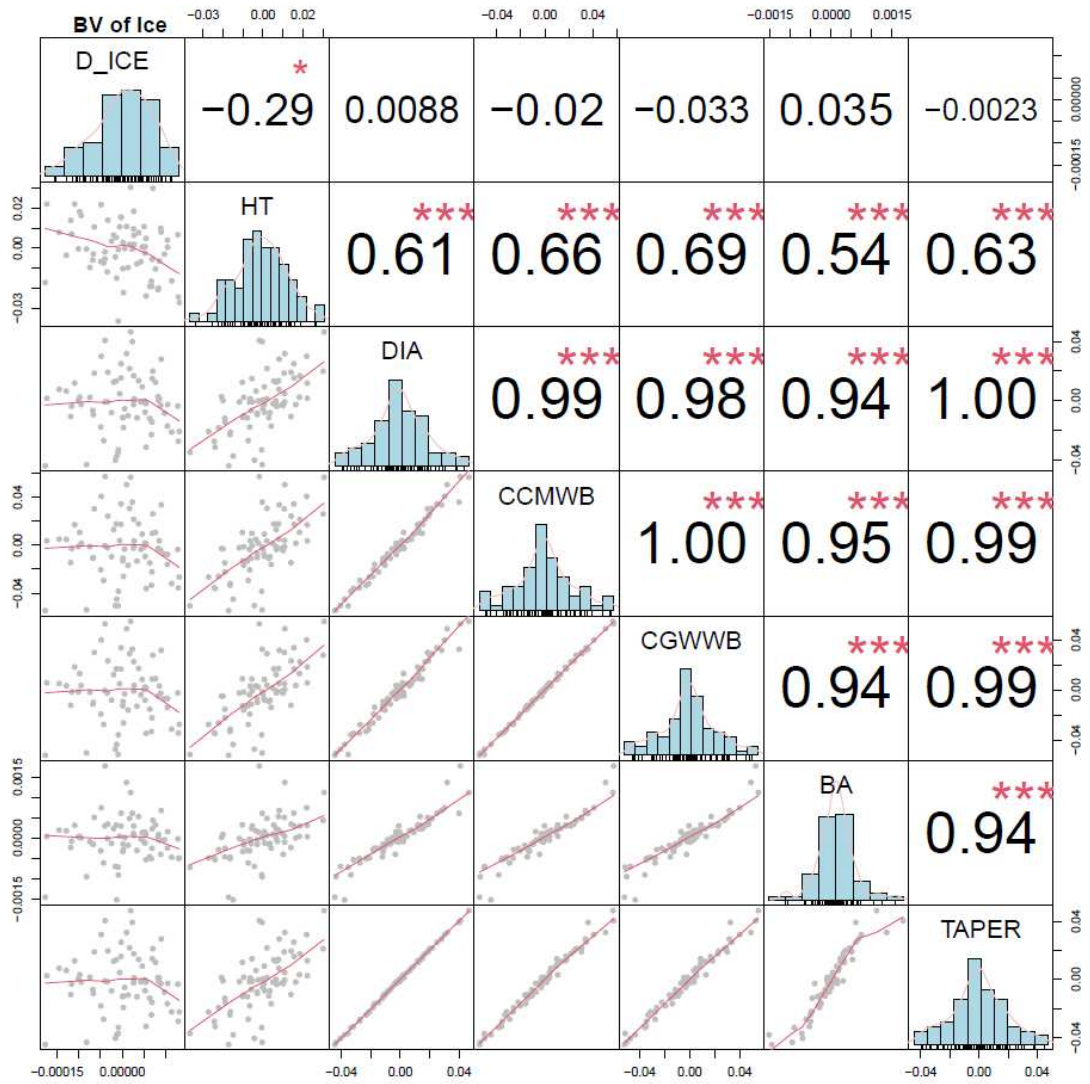

926

927 **Fig. 4.** Correlation and histogram of breeding values for multiple traits in the ice damage zone (11 trials).

928 Note, HT, height (m); DIA, DBH (cm); BA, basal area; HT_RC, height increment from age 5 to 35; CGWWB, complete tree green
929 weight in kilograms of wood, and bark (kg); CCMWB, complete tree cubic meters of wood and bark (m^3); BA, basal area (m^2);
930 D_ICE, ice damage. Pearson's correlation coefficients are in the right upper diagonal, the scatter plots are in the lower-left diagonal
931 for the pairs of physiological variables, while the diagonal are the histograms of each variable. The *p*-values are denoted as following
932 *** < 0.001, ** < 0.01, * < 0.05. HT_RC was only analyzed for the ice zone (11 trials) because the missing value was more than 25%
933 (851/2961= 0.287).

934

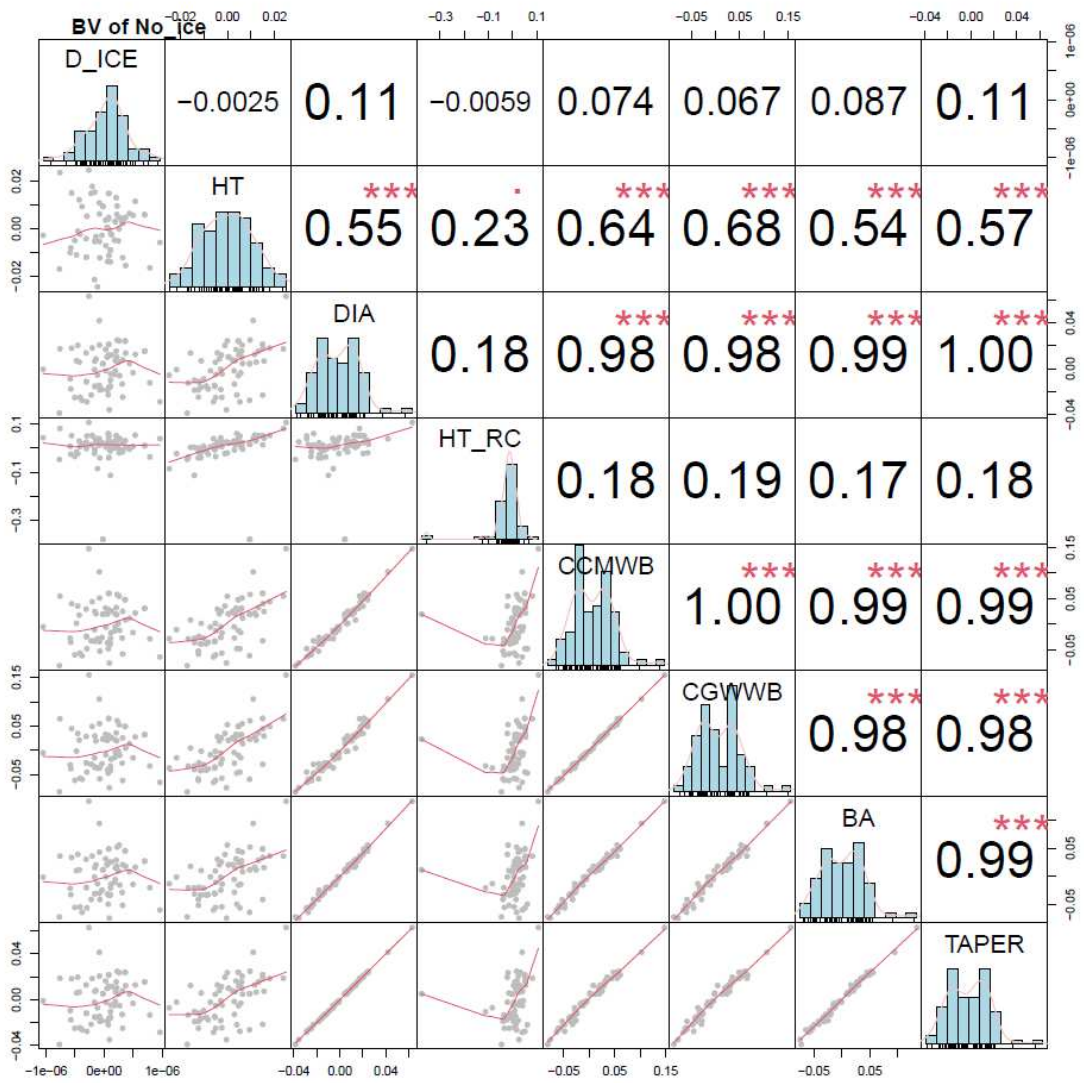

935

936 **Fig. 5.** Pearson correlation, scatter plot, and histogram of breeding values for multiple traits in the non-ice damage zone (4 trials).

937 Note, HT, height (m); DIA, DBH (cm); BA, basal area; HT_RC, height increment from age 5 to 35; CGWWB, complete tree green
938 weight in kilograms of wood, and bark (kg); CCMWB, complete tree cubic meters of wood and bark (m^3); BA, basal area (m^2);
939 D_ICE, ice damage.

940 Pearson's correlation coefficients are in the right upper diagonal, the scatter plots are in the lower-left diagonal for the pairs of
941 physiological variables, while the diagonal are the histograms of each variable. The p-values are denoted as following *** < 0.001,
942 ** < 0.01, * < 0.05.

943

944

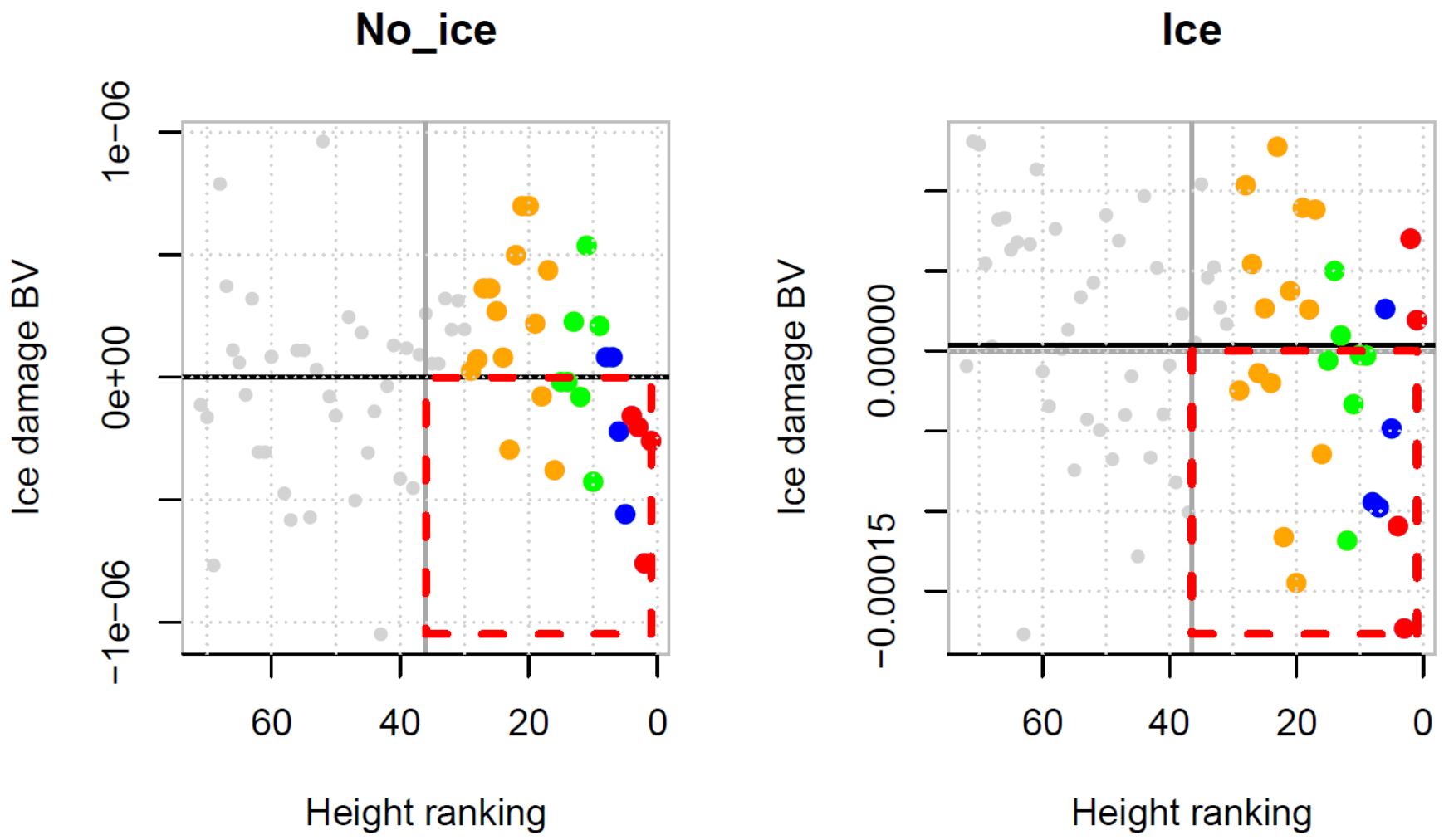

945

946 Fig. 6. Scatter plot of height ranking and the breeding values of ice damage at the no ice zone (4 trials) and the ice damage zone (11
947 trials).

Note, the orange color depicts the top ranked families of volume growth (60 percentiles to 80 percentiles); the green color illustrates the top ranked families from 80 percentiles to 90 percentiles; the blue color shows the families from 90 percentiles to 95 percentiles; the red color depicts the top families above 95 percentiles. The red rectangle captures the candidate families with both genetic gains in growth and frost damage tolerance.

Supplementary materials

Materials and methods appendix 1

The linear model for ice damage is the same as (1) though there are simplified fixed effects by pooling all zones together.

$$y = X\beta + Z_1 a + Z_2 ae + Z_3 d + Z_4 de + Z_5 r + e \text{ (A1)}$$

where the fixed effect is **β** includes the age effect, trial effect nested in age, row effect and column effect nested within the trial-age respectively; block nested within trial-age; the trial effect was excluded because of low significance.

For all MET analyses, heterogeneous variance, and nearest neighbor variance had two dimensional first-order autoregressive (x and y, AR1) variance of residual given $Cov(\varepsilon_{ij}, \varepsilon_{ij'}) = \sigma_\varepsilon^2 Corr(\varepsilon_{ij}, \varepsilon_{ij'}) = \sigma_\varepsilon^2 \rho_j^{|j-j'|} \rho_i^{|i-i'|}$, where σ_ε^2 is the residual variance adjusted with no spatial trend; ε_{ij} is the residual of the individual tree at position (i,j), and ρ is the correlation coefficient at i-direction (row) or j direction (column). R = $\sigma_\varepsilon^2 AR1 + \bigoplus_{i=1}^{i=n} \sigma_{e\,i}^2$ *or* $\sigma_\varepsilon^2 AR1 + \sigma_{e\,i}^2 \otimes I$ where σ_ε^2AR1 is the variance covariance matrix of the spatial residual variance (Bian *et al.*, 2017); AR1 is $\Sigma_{row} \otimes \Sigma_{column}$ containing the correlation coefficients ρ, where Σ_{row} and Σ_{column} are the row and column correlation matrices (De Faveri *et al.*, 2017); for the heterogeneous variances model, the independent residual variance-covariance matrix is as $\bigoplus_{i=1}^{i=n} \sigma_{e\,i}^2$; and R, i, n, are the variance-covariance matrix of the random effects, i[th] index of trial, the total number of trials.

The univariate family (GCA, SCA) models were constructed for estimating other family heritabilities with family terms rather than the individual tree models (1) and A1 (animal model). Comparing to the individual tree model (1) and A1, GCA-SCA model estimates the family means rather than individual tree breeding values (Isik *et al.*, 2017). The details of the function were as follows,

$$y = X\beta + Z_1 f + Z_2 fe + Z_3 m + Z_4 me + Z_5 fam + Z_6 r + e \text{ (A2)}$$

where the fixed effect is **β** including the same effects of the model (A1) for 11 ice storm damage zones, zone effect, trial effect nested in age and zones, row effect and column effect nested within the trial-age-zone respectively; block nested within trial-age-zone; the

zone transfer of male and female parent (provenances) were not fitted in the fixed effect due to the insignificance; *f* denotes the random vector of female general combining capacity (GCA), with f~$N(0, \sigma_f^2 I)$, where σ_f^2 is the female GCA variance; *fe* denotes the random interaction vector of female GCA and environment effects, with fe~$N(0, \sigma_{fe}^2 I)$, where σ_{fe}^2 is the interaction variance of female GCA and environment; *m* is the random male GCA effect, with m~ $N(0, \sigma_m^2 I)$, σ_m^2 denotes the male GCA variance; *me* is the random interaction effect between male GCA and the environment, with *me*~ $N(0, \sigma_{me}^2 I)$, σ_{me}^2 denotes the interaction variance of male GCA x environment; fam is the random specific combining ability (SCA) effect, fam~ $N\left(0, \sigma_{fam}^2 I\right)$, σ_{fam}^2 denotes the SCA variance; r is the random row plot effect nested in the trial r ~ $N\left(0, \sigma_{r(t)}^2 I\right)$ where t is the t[th] block-progeny test site-age-zone combination effect. The residual e has heterogeneous variance-covariance structure, e~$N(0, \bigotimes_{i=1}^{i=n} \sigma_{ei}^2)$ where i is i-th field trial and σ_{ei}^2 is the residual variance of i-th site.

Family mean heritabilities were calculated with the family model (5) with following formulas,

$$\widehat{\sigma_{HS}^2} = \frac{\left(\widehat{\sigma_f^2}+\widehat{\sigma_m^2}\right)}{2} + \frac{\widehat{\sigma_{fam}^2}}{p-1} + \frac{\widehat{\sigma_{fe}^2}+\widehat{\sigma_{me}^2}}{e} + \frac{\widehat{\sigma_e^2}}{ernp-1} \quad (13)$$

$$\widehat{h_{HS}^2} = \frac{(\widehat{\sigma_f^2}+\widehat{\sigma_m^2})/2}{\widehat{\sigma_{HS}^2}} = \frac{(\widehat{\sigma_f^2}+\widehat{\sigma_m^2})/2}{\frac{\left(\widehat{\sigma_f^2}+\widehat{\sigma_m^2}\right)}{2}+\frac{\widehat{\sigma_{fam}^2}}{p-1}+\frac{\widehat{\sigma_{fe}^2}+\widehat{\sigma_{me}^2}}{e}+\frac{\widehat{\sigma_e^2}}{ernp-1}} \quad (14)$$

$$\widehat{\sigma_{FS}^2} = \left(\widehat{\sigma_f^2} + \widehat{\sigma_m^2}\right) + \widehat{\sigma_{fam}^2} + (\widehat{\sigma_{fe}^2} + \widehat{\sigma_{me}^2})/e + \widehat{\sigma_e^2}/ern \quad (15)$$

$$\widehat{h_{FS}^2} = \frac{(\widehat{\sigma_f^2}+\widehat{\sigma_m^2})}{\widehat{\sigma_{FS}^2}} = \frac{(\widehat{\sigma_f^2}+\widehat{\sigma_m^2})}{\left(\widehat{\sigma_f^2}+\widehat{\sigma_m^2}\right)+\widehat{\sigma_{fam}^2}+(\widehat{\sigma_{fe}^2}+\widehat{\sigma_{me}^2})/e+\widehat{\sigma_e^2}/ern} \quad (16)$$

$$\widehat{H_{FS}^2} = \frac{(\widehat{\sigma_f^2}+\widehat{\sigma_m^2}+\widehat{\sigma_{fam}^2})}{\widehat{\sigma_{FS}^2}} = \frac{(\widehat{\sigma_{GF}^2}+\widehat{\sigma_{MF}^2}+\widehat{\sigma_{SCA}^2})}{\left(\widehat{\sigma_f^2}+\widehat{\sigma_m^2}\right)+\widehat{\sigma_{fam}^2}+(\widehat{\sigma_{fe}^2}+\widehat{\sigma_{me}^2})/e+\widehat{\sigma_e^2}/ern} \quad (17)$$

$$\widehat{\sigma^2_{wfs}} = \frac{(e-1)}{e}\left(\widehat{\sigma^2_{fe}} + \widehat{\sigma^2_{me}}\right) + \widehat{\sigma^2_{\bar{e}}}\ (ern-1)/ern \quad (18)$$

$$\widehat{h^2_w} = \frac{(\widehat{\sigma^2_f}+\widehat{\sigma^2_m})}{\widehat{\sigma^2_{wfs}}} = \frac{(\widehat{\sigma^2_f}+\widehat{\sigma^2_m})}{\frac{(e-1)}{e}\left(\widehat{\sigma^2_{fe}}+\widehat{\sigma^2_{me}}\right)+\widehat{\sigma^2_{\bar{e}}}\ (ern-1)/ern} \quad (19)$$

$$\widehat{H^2_w} = \frac{(\widehat{\sigma^2_f}+\widehat{\sigma^2_m}+3\widehat{\sigma^2_{fam}})}{\widehat{\sigma^2_{wfs}}} = \frac{(\widehat{\sigma^2_f}+\widehat{\sigma^2_m}+3\widehat{\sigma^2_{fam}})}{\frac{(e-1)}{e}\left(\widehat{\sigma^2_{fe}}+\widehat{\sigma^2_{me}}\right)+\widehat{\sigma^2_{\bar{e}}}\ (ern-1)/ern} \quad (20)$$

where $\widehat{\sigma^2_{HS}}$ denotes the half-sib mean variance; p is the number of parents in the diallel set; $\widehat{h^2_{HS}}$ is the narrow-sense half-sib mean heritability; $\widehat{\sigma^2_{FS}}$ denotes the full-sib family mean variance; $\widehat{h^2_{FS}}$ is the narrow-sense full-sib mean heritability; $\widehat{H^2_{FS}}$ is the broad-sense full-sib mean heritability; $\widehat{\sigma^2_{wfs}}$ is the within-full-sib-family variance; $\widehat{h^2_w}$ denotes the narrow-sense within-full-sib family heritability; $\widehat{H^2_w}$ is the broad-sense within-full-sib family heritability. The among-plot variance is not considered in the estimates while only the within plot variance $\widehat{\sigma^2_{\bar{e}}}$ was considered. And e is the number of trials; n is the number of trees within each plot for each cross; t is the number of blocks per trial (Xiang *et al.*, 2003a; Isik *et al.*, 2017). The within plot residual e has heterogeneous variance-covariance structure, e~$N(0,\bigotimes_{i=1}^{i=n}\sigma^2_{ei})$ where i is i-th field trial and σ^2_{ei} is the residual variance of i-th trial. $\widehat{\sigma^2_{\bar{e}}}$ is the average of n σ^2_{ei} of trials.

Table appendix 1 *Post-hoc* row and column number of 15 progeny trials

Site	Column	Row
1	66	30
5	68	40
6	67	30
10	102	30
14	64	30
19	69	30
21	67	20
25	85	20
28	32	50
29	80	20
31	79	20
32	42	30
33	35	50
38	25	60
48	148	10

Table appendix 2 Models used in this study.

Model of MET	Scenarios of zones (fixed effect)	Random residual structures
Individual tree model	Ice damage zone	Autoregressive 1 and heterogeneous variance-covariance structure of e $R = \sigma_\varepsilon^2 AR1 + \bigoplus_{i=1}^{i=n} \sigma_{e\,i}^2$
	non ice damage zone	
	Combined zones	
Family model	Ice damage zone	Heterogeneous variance-covariance structure of e $R = \bigoplus_{i=1}^{i=n} \sigma_{e\,i}^2$
	non ice damage zone	
	Combined zones	

Table appendix 3 Comparison of the two types of univariate models deployed

	Advantages	Disadvantages
Individual tree model	Easy to apply for pedigree structure based on the registry and feasible for future genomic selection Estimates of family and individual tree breeding values and genetic values Higher heritability estimates	GxE variance components
Family model	Better estimates on the GxE variance components Better model convergence Better fitting based on slightly lower AIC and BIC	Only estimates the GCA and SCA

For such seedling progeny trials without clone/individuals within families per full-sib family, the family model could overall outperform the individual tree model in the MET analyses.

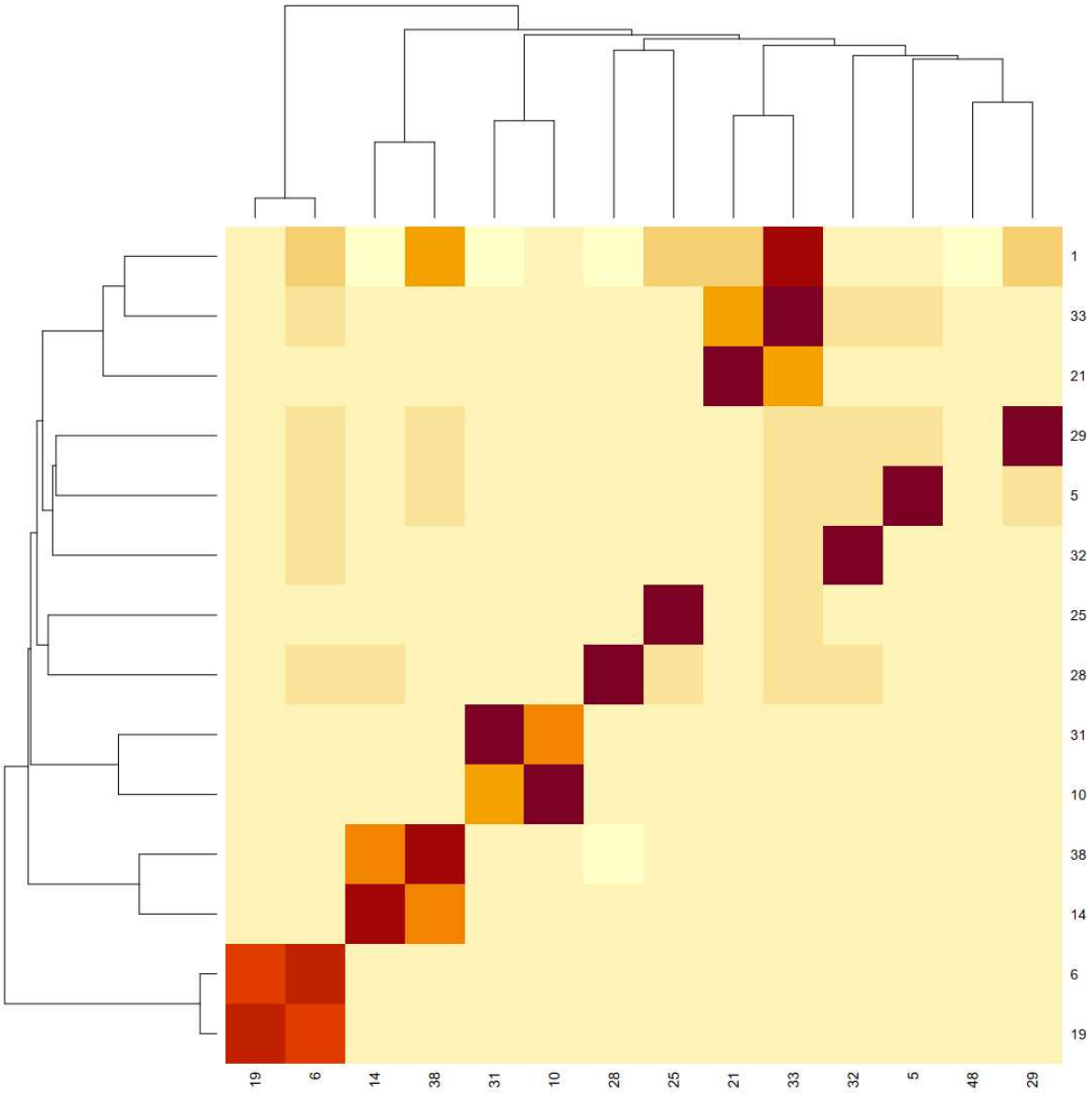
1
33
21
29
5
32
25
28
31
10
38
14
6
19
19
6
14
38
31
10
28
25
21
33
32
5
48
29

1014

Figure Appendix 1 Heatmap showing the connectivity (sharing the same full-sib families) among 15 progeny tests.

1017

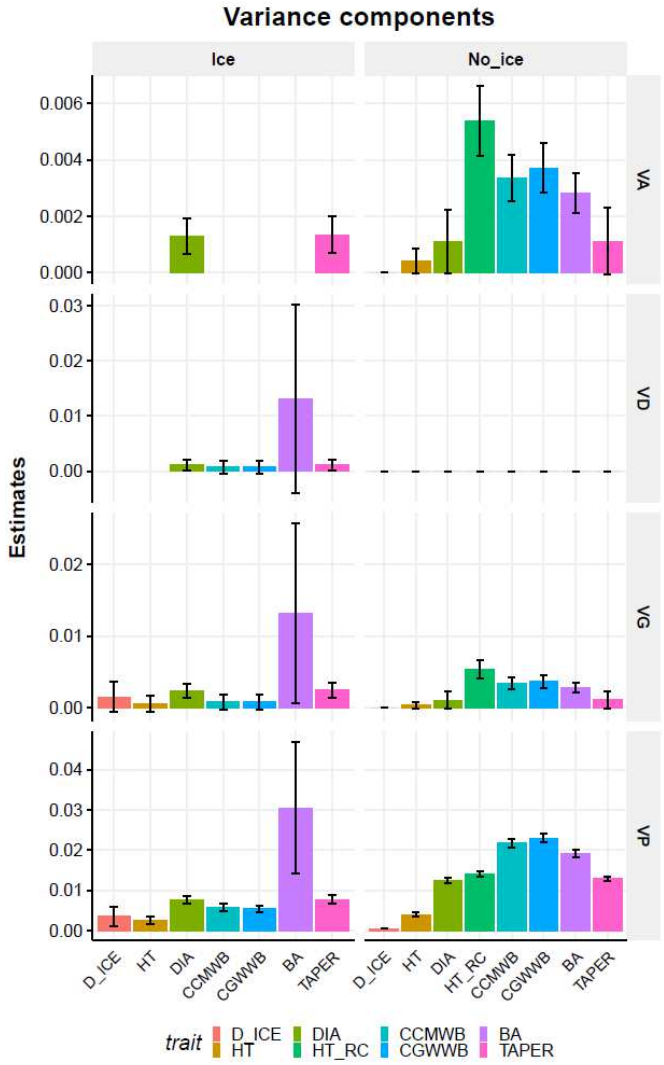

1018

1019 **Figure Appendix 2** Variance components of post-hoc adjusted models (individual tree model).

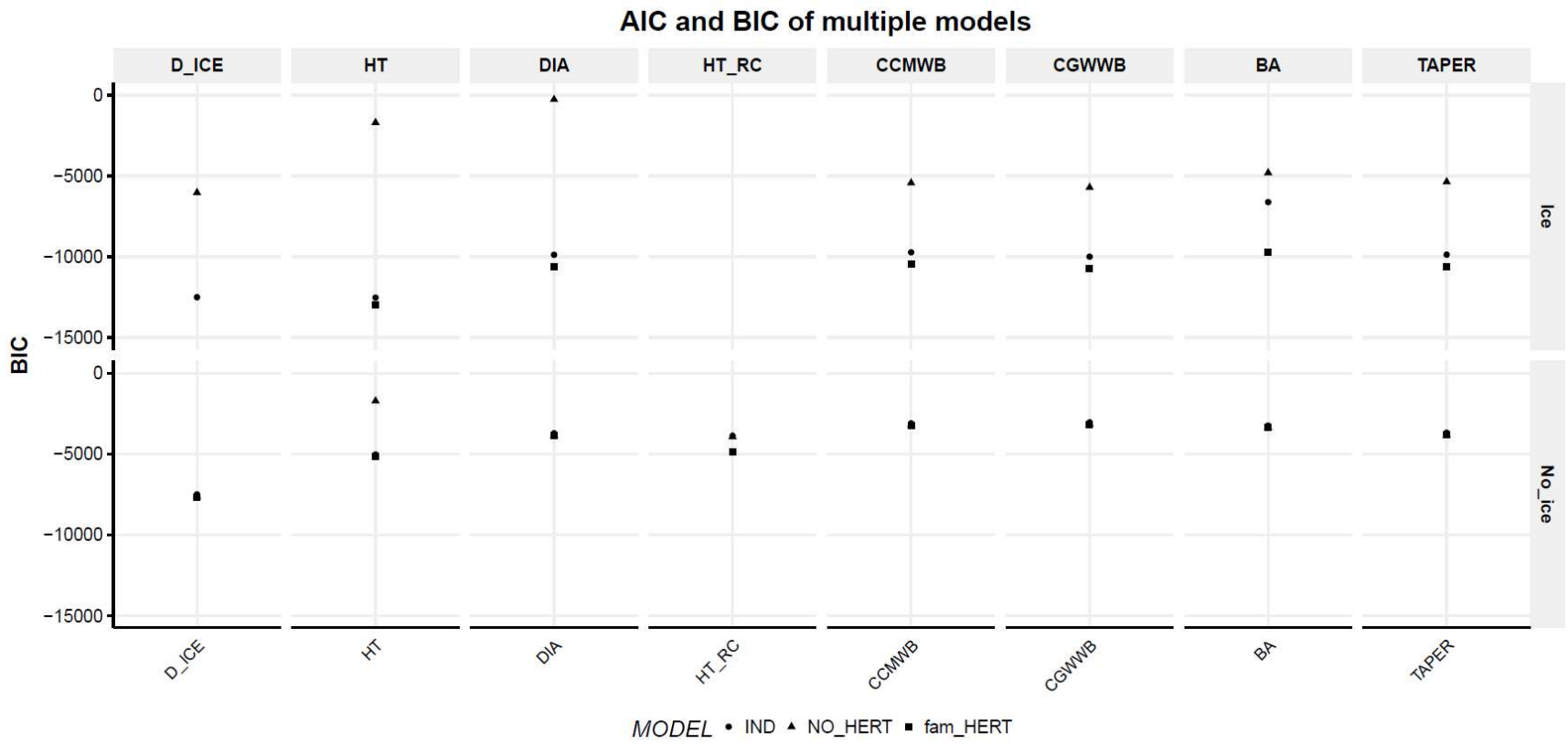

Figure Appendix 3 AIC and BIC of multiple models including individual tree model (IND), simplified individual tree model without post-hoc adjustment (NO_HERT), and family model (fam_HERT).

Table Appendix 4 Genetic parameters of narrow-sense heritability, broad-sense heritability, and family heritability of multiple traits at two zones (ice damage and non-ice)

Trial Condition	Traits	Parameter	Estimates (SE)	Sig.
No Ice	D_ICE	h^2_{HS}	0.981 (0.074)	*
		h^2_{ind}	-	NS
		H^2_B	-	NS
	HT	h2BR_f	0.122 (0.104)	NS
		h2bFS	0.873 (0.133)	*
		h2bw	0.086 (0.081)	NS
		h2ind	0.103 (0.106)	NS
		H^2_B	0.103 (0.106)	NS
	DIA	h2R_f	0.091 (0.087)	NS
		h2BR_f	0.091 (0.087)	NS
		h2HS	0.918 (0.122)	*
		h2FS	0.844 (0.168)	*
		h2bFS	0.845 (0.167)	*
		h2w	0.002 (0.002)	NS
		h2bw	0.025 (0.033)	NS
		h2ind	0.089 (0.091)	NS
		H^2_B	0.089 (0.091)	NS
	HT_RC	h2BR_f	0.159 (0.117)	NS
		h2bFS	0.920 (0.090)	*
		h2bw	0.149 (0.138)	NS
		h2ind	0.384 (0.083)	*
		hb2	0.384 (0.083)	*
	CCMWB	h2R_f	0.091 (0.089)	NS
		h2BR_f	0.091 (0.089)	NS
		h2HS	0.915 (0.127)	*
		h2FS	0.843 (0.171)	*
		h2bFS	0.843 (0.171)	*
		h2w	0.002 (0.002)	NS
		h2bw	0.025 (0.033)	NS
		h2ind	0.156 (0.035)	*
		hb2	0.156 (0.035)	*
	CGWWB	h2R_f	0.092 (0.090)	NS
		h2BR_f	0.092 (0.090)	NS
		h2HS	0.913 (0.129)	*

		h2FS	0.842 (0.173)	*
		h2bFS	0.842 (0.173)	*
		h2w	0.002 (0.002)	NS
		h2bw	0.025 (0.032)	NS
		h2ind	0.162 (0.036)	*
		H^2_B	0.162 (0.036)	*
	BA	h2R_f	0.088 (0.087)	NS
		h2BR_f	0.088 (0.087)	NS
		h2HS	0.914 (0.129)	*
		h2FS	0.839 (0.175)	*
		h2bFS	0.839 (0.175)	*
		h2w	0.002 (0.002)	NS
		h2bw	0.024 (0.032)	NS
		h2ind	0.148 (0.035)	*
		H^2_B	0.148 (0.035)	*
	TAPER	h2R_f	0.089 (0.087)	NS
		h2BR_f	0.089 (0.087)	NS
		h2HS	0.915 (0.126)	*
		h2FS	0.841 (0.172)	*
		h2bFS	0.842 (0.172)	*
		h2w	0.002 (0.002)	NS
		h2bw	0.025 (0.032)	NS
		h2ind	0.087 (0.091)	NS
		H^2_B	0.087 (0.091)	NS
---	---	---	---	---
Ice	D_ICE	h2R_f	-	*
		h2BR_f	0.010 (0.013)	NS
		h2HS	0.048 (0.039)	NS
		h2FS	0.003 (0.001)	*
		h2bFS	0.422 (0.309)	NS
		h2w	-	*
		h2bw	0.015 (0.018)	NS
		H^2_B	0.434 (0.667)	NS
	HT	h2R_f	0.018 (0.021)	NS
		h2BR_f	0.018 (0.021)	NS
		h2HS	0.716 (0.299)	*
		h2FS	0.477 (0.322)	NS
		h2bFS	0.479 (0.321)	NS

		h2w	0.001 (0.001)	NS
		h2bw	0.007 (0.008)	NS
		H^2_B	0.239 (0.393)	NS
	DIA	h2R_f	0.070 (0.046)	NS
		h2BR_f	0.096 (0.042)	*
		h2HS	0.913 (0.085)	*
		h2FS	0.610 (0.270)	*
		h2bFS	0.840 (0.079)	*
		h2w	0.003 (0.002)	NS
		h2bw	0.057 (0.035)	NS
		h2ind	0.170 (0.084)	*
		H^2_B	0.316 (0.094)	*
	CCMWB	h2R_f	0.064 (0.039)	NS
		h2BR_f	0.075 (0.037)	*
		h2HS	0.916 (0.080)	*
		h2FS	0.690 (0.251)	*
		h2bFS	0.807 (0.098)	*
		h2w	0.003 (0.002)	NS
		h2bw	0.038 (0.028)	NS
		H^2_B	0.151 (0.180)	NS
	CGWWB	h2R_f	0.064 (0.038)	NS
		h2BR_f	0.071 (0.037)	NS
		h2HS	0.914 (0.081)	*
		h2FS	0.713 (0.248)	*
		h2bFS	0.799 (0.104)	*
		h2w	0.002 (0.002)	NS
		h2bw	0.034 (0.026)	NS
		H^2_B	0.156 (0.187)	NS
	BA	hRf2	0.066 (0.042)	NS
		h2BR_f	0.088 (0.039)	*
		h2HS	0.918 (0.081)	*
		h2FS	0.625 (0.262)	*
		h2bFS	0.833 (0.081)	*
		h2w	0.003 (0.002)	NS
		h2bw	0.053 (0.033)	NS
		H^2_B	0.432 (0.468)	NS
	TAPER	h2R_f	0.070 (0.046)	NS
		h2BRf	0.095 (0.042)	*

		h2HS	0.910 (0.086)	*
		h2FS	0.621 (0.269)	*
		h2bFS	0.836 (0.082)	*
		h2w	0.003 (0.002)	NS
		h2bw	0.055 (0.035)	NS
		h2ind	0.174 (0.085)	*
		H^2_B	0.319 (0.095)	*

Note, Narrow-sense heritability, broad-sense heritability, and family heritability of multiple traits at two zones (ice damage versus non-ice). Ice is zone with ice damage (11 trials); Non-ice zone without ice damage; h2ind, narrow-sense heritability of individual tree model; H^2_B, broad-sense heritability of the individual tree model; h2R_f, narrow-sense heritability of the family model; h2BR_f, broad-sense heritability of the family model; h2HS, narrow-sense half-sib family mean heritability; h2FS, narrow-sense full-sib family mean heritability; h2bFS, broad-sense full-sib family heritability; h2w, narrow-sense within-family heritability; h2bw, broad-sense within-family heritability; HT, height (m); DIA, DBH (cm); BA, basal area (m2); HT_RC, height increment from age 5 to 35; CGWWB, complete tree green weight in kilograms of wood, and bark (kg); CCMWB, complete tree cubic meters of wood and bark (m3); D_ICE, ice damage. Missing estimates are due to no convergence of the linear mixed model. (*) denotes $P < 0.05$; NS denotes non-significant.

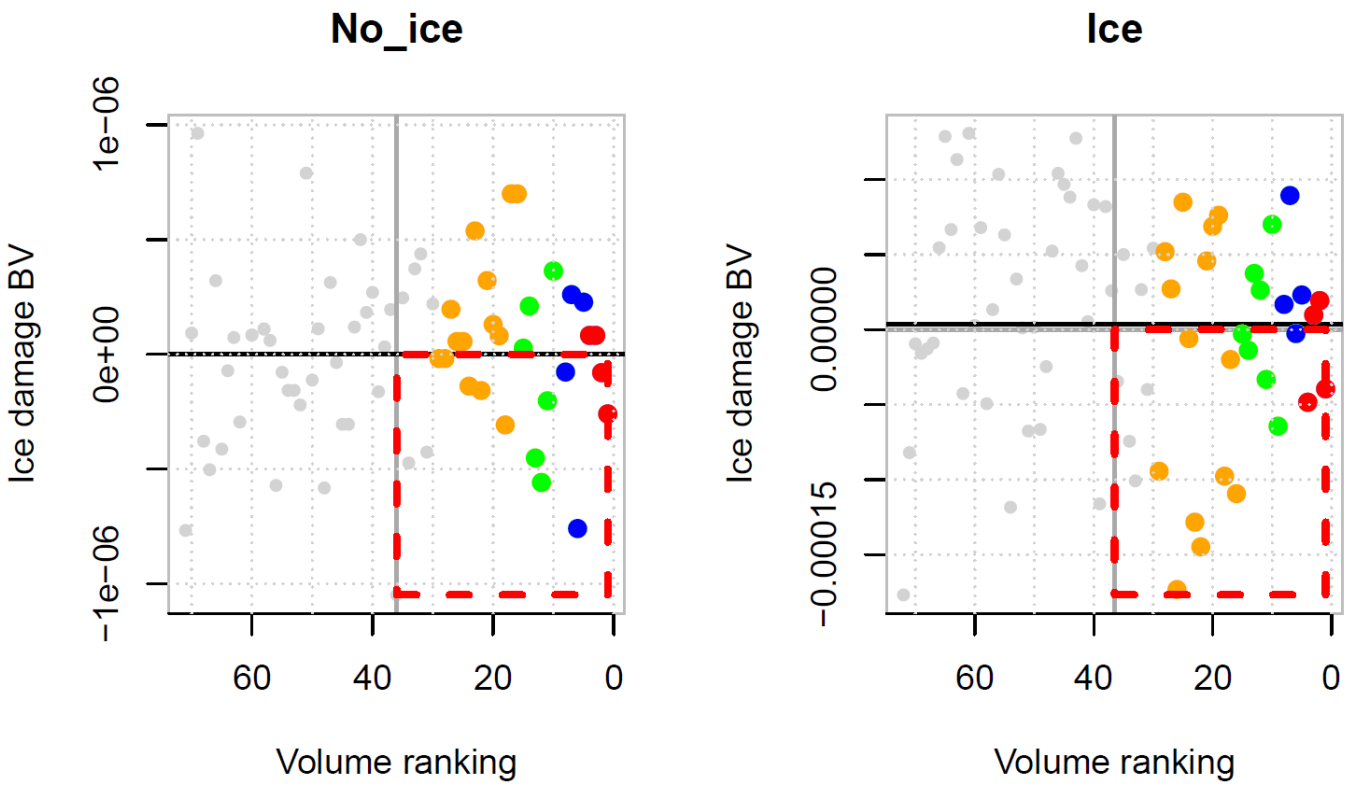

Figure Appendix 5. Scatter plot of volume ranking and the breeding values of ice damage in the non-ice zone (4 trials) and the ice damage zone (11 trials).

Note, the orange color depicts the top ranked families of volume growth (60 percentiles to 80 percentiles); the green color illustrates the top ranked families from 80 percentiles to 90 percentiles; the blue color shows the families from 90 percentiles to 95 percentiles; the red color depicts the top families above 95 percentiles. The red rectangle captures the candidate families with both genetic gains in growth and frost damage tolerance.